



Search for heavy resonances decaying to WW , WZ , or WH boson pairs in the lepton plus merged jet final state in proton-proton collisions at $\sqrt{s} = 13$ TeV

The CMS Collaboration*

Abstract

A search for new heavy resonances decaying to pairs of bosons (WW , WZ , or WH) is presented. The analysis uses data from proton-proton collisions collected with the CMS detector at a center-of-mass energy of 13 TeV, corresponding to an integrated luminosity of 137 fb^{-1} . One of the bosons is required to be a W boson decaying to an electron or muon and a neutrino, while the other boson is required to be reconstructed as a single jet with mass and substructure compatible with a quark pair from a W , Z , or Higgs boson decay. The search is performed in the resonance mass range between 1.0 and 4.5 TeV and includes a specific search for resonances produced via vector boson fusion. The signal is extracted using a two-dimensional maximum likelihood fit to the jet mass and the diboson invariant mass distributions. No significant excess is observed above the estimated background. Model-independent upper limits on the production cross sections of spin-0, spin-1, and spin-2 heavy resonances are derived as functions of the resonance mass and are interpreted in the context of bulk radion, heavy vector triplet, and bulk graviton models. The reported bounds are the most stringent to date.

Submitted to Physical Review D

1 Introduction

The standard model (SM) of particle physics [1–3] has successfully accommodated a multitude of experimental observations, culminating in the discovery of a Higgs boson (H) [4–6]. Yet, the SM falls short of addressing several outstanding issues, such as the hierarchy problem, i.e., explaining the large difference between the Higgs boson mass and the largest scale in the SM, that are necessary components of a consistent theory of nature up to the Planck scale. These shortcomings are addressed by a variety of theoretical extensions to the SM, several of which predict the existence of new heavy particles with masses near the TeV scale that couple to W, Z, or Higgs bosons and could be produced in proton-proton (pp) collisions at the CERN Large Hadron Collider (LHC). Commonly probed models include the bulk scenario of the Randall–Sundrum (RS) model with warped extra dimensions [7, 8] and examples of the heavy vector triplet (HVT) framework [9], which generically represents a number of models that predict additional gauge bosons, such as composite Higgs [10–14] and little Higgs [15, 16] models.

In this paper, a search is presented for a heavy resonance X with mass between 1.0 and 4.5 TeV decaying to a pair of bosons, using pp collision data at a center of mass energy of 13 TeV, collected with the CMS detector from 2016 to 2018. The final state considered targets the scenario where one of the two bosons is required to be a W boson decaying to an electron or muon and a neutrino, while the other boson is either a W or Z boson (collectively referred to as V) decaying to a quark pair ($q\bar{q}^{(\prime)}$) or a Higgs boson decaying to a bottom quark pair ($b\bar{b}$).

A boosted V or Higgs boson with $p_T \approx 250$ GeV and mass $m \approx 100$ GeV decaying to quarks is expected to have its decay products within a cone of $\Delta R = \sqrt{(\Delta\eta)^2 + (\Delta\phi)^2} \approx 2m/p_T \approx 0.8$. Therefore, in this search targeting TeV resonances, we expect the hadronically decaying boson to appear as a single broad massive jet. The search targets resonance production via gluon-gluon fusion (ggF) and Drell–Yan-like quark-antiquark annihilation (DY) processes, where no other decay products are expected, as well as production via vector boson fusion (VBF), where the final state contains two additional quark-induced jets in the forward and backward regions of the detector. Example Feynman diagrams for three representative combinations of production mechanisms and final states studied in this paper are shown in Fig. 1.

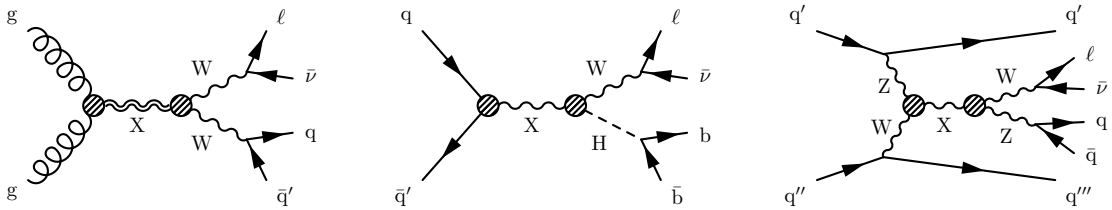


Figure 1: Feynman diagrams for three of the processes studied in this paper: (left) ggF-produced, spin-2 resonance decaying to $WW \rightarrow \ell\nu q\bar{q}'$; (center) DY-like, charged spin-1 resonance decaying to $WH \rightarrow \ell\nu b\bar{b}$; (right) VBF-produced, charged spin-1 resonance decaying to $WZ \rightarrow \ell\nu q\bar{q}$.

Previous searches for heavy WW and WZ resonances in semileptonic final states by the ATLAS [17–19] and CMS [20–22] Collaborations using LHC data collected in 2012, 2015, and 2016, as well as the recent ATLAS search with the complete 2015–2018 data set [23], have not observed any statistically significant deviations from the SM background expectation and have set increasingly stringent upper bounds on resonance production cross sections. In parallel, searches for semileptonically decaying WH resonances have been reported by ATLAS [24–26] and CMS [27–29] in a separate series of publications and have yielded similar outcomes.

Compared to the previous CMS search for semileptonic WW and WZ resonances with 2016 data [22], this analysis still employs a signal extraction procedure based on a two-dimensional (2D) maximum likelihood fit, but extends the search sensitivity to WH decays and VBF production modes by employing $b\bar{b}$ tagging and VBF tagging. In addition, sensitivity to the spin of the resonance is introduced for the first time, boosting the sensitivity of the search beyond the improvement expected by the larger data sample.

The fit is performed in the plane whose coordinates are defined by the invariant mass of the reconstructed diboson system and by the mass of its $V \rightarrow q\bar{q}^{(\prime)}$ or $H \rightarrow b\bar{b}$ jet component. The dominant SM backgrounds to this search arise from $W + \text{jets}$ production, single and pair production of top quarks, and SM diboson production, all of which can produce lepton plus jets events where the jets either originate from boosted, hadronically decaying vector bosons or are ordinary quark- or gluon-initiated jets. The 2D fit strategy improves the search sensitivity across a large range of resonance masses, making the analysis flexible by enabling a simultaneous search for WW , WZ , and WH resonances using the same background estimation procedure for all final states and production mechanisms.

2 The CMS detector and event reconstruction

The central feature of the CMS apparatus is a superconducting solenoid of an internal diameter of 6 m that provides a magnetic field of 3.8 T. Within the solenoid volume are a silicon pixel and strip tracker, a lead tungstate crystal electromagnetic calorimeter (ECAL), and a brass and scintillator hadron calorimeter (HCAL), each composed of a barrel and two endcap sections. Forward calorimeters extend the pseudorapidity coverage provided by the barrel and endcap detectors. Muons are detected in gas-ionization chambers embedded in the steel flux-return yoke outside the solenoid. A more detailed description of the CMS detector, together with a definition of the coordinate system used and the relevant kinematic variables, can be found in Ref. [30].

Event reconstruction relies on the particle-flow (PF) algorithm [31], which aims to identify each individual particle with an optimized combination of information from the various elements of the CMS detector. The energy of photons is obtained from the ECAL measurement. The energy of electrons is determined from a combination of the electron momentum at the primary interaction vertex as determined by the tracker, the energy of the corresponding ECAL cluster, and the energy sum of all bremsstrahlung photons spatially compatible with originating from the electron track. The momentum of muons is obtained from the combined curvature of the corresponding track in both silicon tracker and the muon system. The energy of charged hadrons is determined from a combination of their momentum measured in the tracker and the matching ECAL and HCAL energy deposits, corrected for the response function of the calorimeters to hadronic showers. Finally, the energy of neutral hadrons is obtained from the corresponding corrected ECAL and HCAL energies. The missing transverse momentum vector \vec{p}_T^{miss} is computed as the negative vector sum of the transverse momenta of all the PF candidates in an event, and its magnitude is denoted as p_T^{miss} [32].

For each event, hadronic jets are clustered from these reconstructed particles using the infrared- and collinear-safe anti- k_T algorithm [33, 34]. The jet momentum is determined as the vector sum of all particle momenta in the jet and is found from simulation to be, on average, within 5 to 10% of the true momentum over the entire p_T spectrum and detector acceptance. Jet energy corrections are derived from simulation studies so that the average measured response of jets becomes identical to that of particle-level jets [35].

Additional pp interactions within the same or nearby bunch crossings (pileup) can contribute additional tracks and calorimetric energy depositions, increasing the apparent jet momentum. To mitigate this effect, tracks identified to be originating from pileup vertices are discarded and an offset correction is applied to correct for remaining contributions [31, 34]. In the computation of jet substructure variables, a different Pileup-Per Particle Identification (PUPPI) algorithm [36, 37], which uses local shape information of charged pileup to rescale the momentum of each particle based on its compatibility with the primary interaction vertex, is employed.

Events of interest are initially selected using a two-tiered trigger system. The first level, composed of custom hardware processors, uses information from the calorimeters and muon detectors to select events at a rate of around 100 kHz within a fixed latency of about 4 μ s [38]. The second level, known as the high-level trigger (HLT), consists of a farm of processors running a version of the full event reconstruction software optimized for fast processing and reduces the event rate to around 1 kHz before data storage [39].

3 Data and simulated samples

This search uses data samples of pp collisions collected by the CMS experiment at the LHC at a center-of-mass energy of 13 TeV. The data were collected in 2016, 2017, and 2018, and correspond to integrated luminosities of 35.9 fb⁻¹, 41.5 fb⁻¹, and 59.7 fb⁻¹, respectively. The performance of the detector on the variables of interest was very similar in the different periods of data taking, therefore they are treated as one single data set, with a total integrated luminosity of 137 fb⁻¹. Collision events are selected mainly by HLT algorithms that either require the reconstruction of an electron within $|\eta| < 2.5$ or a muon within $|\eta| < 2.4$.

Several electron triggers are combined. In 2016, three p_T thresholds of 27, 55, and 115 GeV are used in association with tight, loose, or no isolation criteria, respectively. In 2017 and 2018, two thresholds of 32 and 115 GeV are used with tight or no isolation. Muon triggers have a p_T threshold of 50 GeV. To further increase the trigger efficiency, another algorithm selects events with $p_T^{\text{miss}} > 120$ GeV, exploiting the presence of the high- p_T neutrino in the $W \rightarrow \ell\nu$ decay. The overall HLT efficiency is larger than 99.7% for signal events passing the offline selection described in Section 4.

Several signal benchmark scenarios are used to interpret the results of the search, focusing on relevant models probed in earlier searches by the ATLAS and CMS Collaborations. Spin-0 radions [40–42] and spin-2 gravitons [43–45] decaying to WW are generated for the bulk scenario of the RS model of warped extra dimensions [7, 8]. For bulk gravitons, denoted as G_{bulk} , the ratio \tilde{k} of the unknown curvature scale of the extra dimension k and the reduced Planck mass \bar{M}_{Pl} is set to $\tilde{k} = 0.5$, which ensures that the natural width of the graviton is negligible with respect to the experimental resolution [46]. For bulk radions, we consider a scenario with $kr_c\pi = 35$ and $\Lambda_R = 3$ TeV, where r_c is the compactification radius and Λ_R is the ultraviolet cutoff of the theory [46]. Spin-1 resonances decaying to WW, WZ, or WH are studied within the HVT framework in the benchmark model B (DY production) [9] and model C (VBF). The HVT framework introduces a triplet of heavy vector bosons with similar masses, of which one is neutral (Z') and two are electrically charged (W'^{\pm}). HVT benchmark models are expressed in terms of a few parameters: the strength c_F of the couplings to fermions, the strength c_H of the couplings to the Higgs boson and to longitudinally polarized SM vector bosons, and the interaction strength g_V of the new vector boson. In HVT model B ($g_V = 3$, $c_H = -0.98$, $c_F = 1.02$) [9], the new resonances are narrow and have large branching fractions to vector boson pairs, while the fermionic couplings are suppressed. In model C ($g_V \approx 1$, $c_H \approx 1$,

$c_F = 0$), the fermionic couplings are zero, and the resonances are produced only through VBF and decay exclusively to pairs of SM bosons. Monte Carlo (MC) simulated samples for bulk radions, bulk gravitons, and resonances of the HVT models are generated at leading order (LO) in quantum chromodynamics (QCD) with MADGRAPH5_aMC@NLO versions 2.2.2 and 2.4.2 [47]. For each model, resonance masses in the range 1.0–4.5 TeV are considered, and the resonance width is set to 0.1% of the resonance mass, ensuring that the width of the signal distribution is dominated by the detector resolution.

Simulated samples for SM background processes are used to optimize the search and to build background templates, as described in Section 5.2. The $W(\rightarrow \ell\nu) + \text{jets}$ process is produced with MADGRAPH5_aMC@NLO at LO in QCD. The background from top quark pair events ($t\bar{t}$) is generated with POWHEG v2 [48–51] at next-to-LO (NLO). Single top quark events are generated in the t channel and associated tW channel at NLO with POWHEG v2 [52, 53], while SM diboson processes are generated at NLO with MADGRAPH5_aMC@NLO using the FxFx merging scheme [54] for WZ and ZZ, and with POWHEG v2 for WW [55].

Parton showering and hadronization are performed with PYTHIA 8.205 (8.230) [56] for 2016 (2017 and 2018) detector conditions. The NNPDF 3.0 [57] parton distribution functions (PDFs) are used together with the CUETP8M1 [58] underlying event tune for 2016 conditions (except for $t\bar{t}$ samples, which use CUETP8M2 [59]), while the NNPDF 3.1 [60] PDFs and the CP5 [61] tune are used for 2017 and 2018 conditions. To simulate the effect of pileup, additional minimum bias interactions are superimposed on the hard-scattering process, and the events are then weighted to match the distributions of the number of pileup interactions observed in 2016, 2017, and 2018 data separately. All samples are processed through a simulation of the CMS detector based on GEANT4 [62] and are reconstructed using the same algorithms used for collision data. Simulated events are also reweighted to correct for differences between data and simulation in the efficiencies of the trigger, lepton identification, and b tagging algorithms described in Section 4.

4 Event selection and categorization

The event selection is designed to isolate events containing a boosted topology consistent with the semileptonic decay of a WW, WZ, or WH pair, involving one energetic electron or muon, large p_T^{miss} , and a so-called large-radius jet corresponding to a W, Z, or Higgs boson candidate.

Electron and muon candidates are considered if they satisfy $p_T > 55 \text{ GeV}$, the same η acceptance requirements as at the HLT, and a set of lepton reconstruction quality and lepton identification requirements optimized to maintain a large efficiency for high-momentum leptons [63, 64]. The electrons must satisfy requirements on the ratio of the energies deposited in the HCAL and ECAL, the distribution of the ECAL deposits, their geometrical matching with reconstructed tracks, and the number of reconstructed hits in the silicon tracker. To reject backgrounds from beauty and charm decays, decays in flight, and misidentified leptons inside jets, muons and electrons are required to be isolated in the detector in a region defined by a cone of $\Delta R < 0.3$ around the respective lepton. The muon isolation variable, defined as the p_T sum of all particles within $\Delta R = 0.3$ of the muon direction, subtracting the muon itself and pileup contributions, is required to be less than 5% of the muon p_T , while electron isolation is defined by applying separate requirements suitable for high energy electrons using the tracker and the calorimeter deposits [63]. Additional requirements on the impact parameters of electron and muon tracks with respect to the primary interaction vertex are applied to suppress the contributions from secondary decays and pileup interactions. The lepton selection requirements

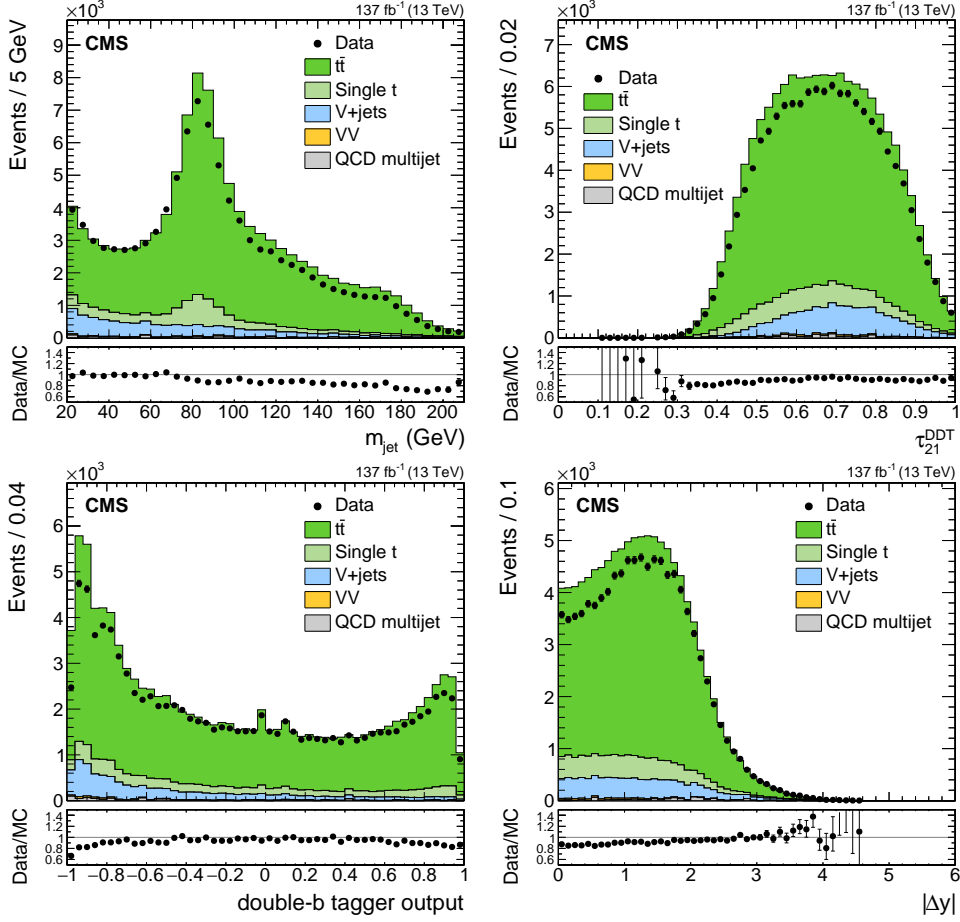


Figure 2: Uncorrected distributions of the soft-drop jet mass m_{jet} (upper left), mass-decorrelated N -subjettiness ratio τ_{21}^{DDT} (upper right), double- b tagger output (lower left), and difference in rapidity $|\Delta y|$ between the reconstructed bosons (lower right), for data and simulated events in the top quark enriched control region. The lower panels show the ratio of the data to the simulation. No event categorization is applied. The events with $\tau_{21}^{\text{DDT}} > 0.80$ are not shown in any distribution other than τ_{21}^{DDT} itself. The vertical bars correspond to the statistical uncertainties of the data.

used establish an identification efficiency of about 90% while ensuring negligible contributions from SM events composed uniquely of jets produced through the strong interaction, referred to as QCD multijet events.

Large-radius jets are clustered using a distance parameter $R = 0.8$ in the anti- k_T algorithm and are required to have $p_T > 200$ GeV. Since the signal is expected to be produced centrally, large-radius jets are required to be in the tracker acceptance ($|\eta| < 2.5$) so as to exploit the maximum granularity of the CMS detector. Another collection of jets is clustered using $R = 0.4$ and referred to as standard jets, with $p_T > 30$ GeV and $|\eta| < 4.7$. Both sets of jets are required to pass tight identification requirements [65]. Large-radius jets located within $\Delta R < 1.0$ of a selected lepton are discarded, as are standard jets located within $\Delta R < 0.8$ of a large-radius jet or within $\Delta R < 0.4$ of a selected lepton.

To identify large-radius jets as hadronic decays of boosted W , Z , and Higgs bosons, jet substructure techniques are employed. First, to perform jet grooming, i.e. to remove soft, wide-angle radiation from the jet, the modified mass-drop algorithm [66, 67] known as “soft drop”

is used with angular exponent $\beta = 0$, soft cutoff threshold $z_{\text{cut}} = 0.1$, and characteristic radius $R_0 = 0.8$ [68]. The invariant mass of the remaining jet constituents is called the soft-drop jet mass, denoted as m_{jet} , and is one of the two observables of the final 2D fit. Second, a V tagging algorithm is defined based on the N -subjettiness ratio between 2-subjettiness and 1-subjettiness [69], $\tau_{21} = \tau_2/\tau_1$, which takes lower values for jets coming from two-prong W, Z , or H decays than for one-prong jets from dominant SM backgrounds. However, the selection on τ_{21} is found to sculpt the distribution of m_{jet} , affecting the monotonically falling behavior of the $W + \text{jets}$ background distributions. Therefore, to decorrelate τ_{21} from the jet mass, the “designing decorrelated taggers” (DDT) procedure [70] is followed, leading to the definition of the mass-decorrelated N -subjettiness ratio $\tau_{21}^{\text{DDT}} \equiv \tau_{21} - M \log(m_{\text{jet}}^2/(p_T \mu))$, with $M = -0.08$ and $\mu = 1 \text{ GeV}$ and using the p_T of the original jet. In the computation of both m_{jet} and τ_{21}^{DDT} , pileup mitigation relies on the PUPPI algorithm. Third, to discriminate $H \rightarrow b\bar{b}$ and $Z \rightarrow b\bar{b}$ decays from other signals and backgrounds that involve light-flavor jets, the so-called double-b tagger is used [71], which is a multivariate discriminant that combines information from displaced tracks, secondary vertices (SV), and the two-SV system within the Higgs or Z boson jet candidate.

The collection of standard jets serves two purposes. First, the b jet identification algorithm known as DeepCSV [71], which relies on a deep neural network that uses track and SV information is applied to standard jets found within $|\eta| < 2.5$. The medium operating point of this algorithm has an efficiency of about 68% for correctly identifying b jets in simulated $t\bar{t}$ events, and a misidentification probability of about 1% for light-flavor jets. Events where at least one standard jet passes this operating point are discarded, thereby reducing the background from events involving top quark decays, and are used to define a top quark enriched control region. Second, events containing at least two standard jets are used to make the search sensitive to VBF-produced resonances. A VBF tagging criterion is defined as $m_{jj}^{\text{VBF}} > 500 \text{ GeV}$ and $|\Delta\eta_{jj}^{\text{VBF}}| > 4$, where m_{jj}^{VBF} and $|\Delta\eta_{jj}^{\text{VBF}}|$ are the invariant mass and pseudorapidity separation of the two highest p_T standard jets. The selection requirements were chosen to reject backgrounds from additional jets present in energetic top events and W production in association with multiple jets. This criterion is used to define additional categories.

The event selection requires the presence of exactly one identified electron or muon, and events that contain additional electrons (muons) passing $p_T > 35$ (20) GeV and otherwise identical requirements are discarded. The p_T^{miss} in the event is required to be greater than 80 GeV if the selected lepton is an electron and greater than 40 GeV if the selected lepton is a muon. Muons have lower QCD background and are not included in the p_T^{miss} calculation in the trigger, resulting in the reconstruction of the whole boosted leptonic W decay as p_T^{miss} , achieving higher efficiency at lower offline thresholds. To reconstruct a $W \rightarrow \ell\nu$ boson candidate, the \vec{p}_T^{miss} is taken as an estimate of the \vec{p}_T of the neutrino, and the longitudinal component p_z of the neutrino momentum is estimated by imposing a W boson mass constraint to the lepton+neutrino system. This leads to a quadratic equation, of which the solution with smallest magnitude of the neutrino p_z is chosen. When no real solution is found, only the real part of the two complex solutions is considered. Besides this leptonically decaying W boson candidate, hereafter referred to as W_{lep} , the hadronically decaying W, Z , or Higgs boson candidate is defined as the most energetic large-radius jet in the event and referred to as V_{had} . The V_{had} is required to pass $\tau_{21}^{\text{DDT}} \leq 0.8$, and the W_{lep} and V_{had} are both required to have $p_T > 200 \text{ GeV}$. They are then combined to form a WW, WZ , or WH diboson candidate, of which the invariant mass is denoted as m_{WV} .

Angular criteria are applied in order to select a diboson-like topology: the angular distance

between the selected lepton and the V_{had} is required to be $\Delta R > \pi/2$, while the difference in azimuthal angle between the V_{had} and both the \vec{p}_T^{miss} and the W_{lep} directions is required to be $|\Delta\phi| > 2$. The difference in rapidity between the W_{lep} and the V_{had} is denoted as $|\Delta y|$ and is used later for event categorization to exploit the fact that signal models investigated in this search tend to have lower values of $|\Delta y|$ compared to backgrounds, except for spin-1 and spin-2 VBF-produced resonances, which significantly populate the $|\Delta y| > 1$ region.

The signal region for the 2D fit is defined by two final requirements on the diboson reconstructed mass and soft-drop jet mass, namely $0.7 < m_{WV} < 6 \text{ TeV}$ and $20 < m_{\text{jet}} < 210 \text{ GeV}$. The lower bound on m_{WV} ensures that the backgrounds have a falling spectrum while allowing a search for resonances with masses greater than 1 TeV, and the 6 TeV upper bound ensures that all observed events are included. The use of a large window for m_{jet} allows the selection of background events containing V jets as well as top quark jet candidates, while retaining sizeable low- and high-mass sidebands to constrain shapes and normalizations. The overall signal selection efficiency times acceptance ranges from 22 to 79%, depending on the benchmark model and increasing with resonance mass.

Table 1: Summary of the categorization scheme in the analysis. The 24 analysis categories are defined by all possible combinations of the criteria defined in each column.

lepton	purity	$b\bar{b}$ /VBF tagging	spin
muon	HP: $\tau_{21}^{\text{DDT}} \leq 0.5$	VBF: $m_{\text{jj}}^{\text{VBF}} > 500 \text{ GeV}$ and $ \Delta\eta_{\text{jj}}^{\text{VBF}} > 4$	LDy: $ \Delta y \leq 1$
electron	LP: $0.5 < \tau_{21}^{\text{DDT}} \leq 0.8$	no- $b\bar{b}$: no VBF and double-b tagger ≤ 0.8 $b\bar{b}$: no VBF and double-b tagger > 0.8	HDy: $ \Delta y > 1$

To enhance the analysis sensitivity to all signals under consideration, each event of the signal region is eventually assigned to one of 24 mutually exclusive search categories, based on a combination of four criteria. First, the event sample is split according to lepton flavor, distinguishing the electron and muons channels, which helps account for the differences in lepton reconstruction and selection. Second, the V tagging information is used to split each channel into a high-purity (HP) and a low-purity (LP) subchannel, which correspond to values of the mass-decorrelated N -subjettiness ratio in the ranges $\tau_{21}^{\text{DDT}} \leq 0.5$ and $0.5 < \tau_{21}^{\text{DDT}} \leq 0.8$, respectively. Third, each subchannel is further divided into three regions, referred to as VBF-tagged for events that satisfy the aforementioned VBF tagging criterion, double-b -tagged ($b\bar{b}$) for non-VBF-tagged events for which the double-b tagger output is larger than 0.8, and non-double-b -tagged (no- $b\bar{b}$) for the remaining events. Fourth, each of the twelve resulting regions is split into two event categories: LDy, corresponding to a difference in rapidity between the reconstructed bosons of $|\Delta y| \leq 1$; and HDy, which corresponds to $|\Delta y| > 1$. The categorization requirements are summarized in Table 1. Besides the signal region, a disjoint event sample enriched in $t\bar{t}$ events with similar kinematic distributions is defined by requiring the presence of a b-tagged standard jet instead of vetoing it. This control region is used to compare data and simulation for the main selection variables, to correct background yields and m_{jet} shapes in the signal region, and to compute efficiency scale factors for the τ_{21}^{DDT} selection. Figure 2 shows the distributions of m_{jet} , τ_{21}^{DDT} , the double-b tagger, and $|\Delta y|$ in this top quark-enriched sample before the aforementioned corrections and scale factors are applied.

5 Two-dimensional templates

A similar signal extraction strategy is followed as in the previous CMS search for semileptonic WV resonances with 2016 data [22], using a simultaneous maximum likelihood fit to the (m_{WV} ,

m_{jet}) data distributions in the 24 search categories. Signal and background templates are constructed using simulated events, after applying corrections to the simulation. Analytical shapes are used to model the signal, while binned templates are used for background processes. The binning was optimized to maximize the number of bins while ensuring smooth templates in all categories. This process resulted in two binning schemes, one for higher statistics and one for lower statistics categories, respectively. Particular care is devoted to constructing smooth background templates, modifying the strategy to accommodate the larger 2D signal region and the fact that new categorization criteria such as VBF tagging and double-b tagging cause some categories to be sparsely populated by simulated events.

5.1 Signal modeling

The 2D probability density function (pdf) for signal events in the (m_{WV}, m_{jet}) plane is described as the product of two one-dimensional (1D) resonant pdfs:

$$P_{\text{sig}}(m_{WV}, m_{\text{jet}}) = P(m_{WV} | m_{\chi}, \theta) P(m_{\text{jet}} | m_{\chi}, \theta),$$

where θ represents sets of nuisance parameters affecting the shape, which we describe in Section 6.2. Each factor in this formula is constructed by fitting a double-sided Crystal Ball (dCB) function [72], composed of a Gaussian core and asymmetric power-law tails, to the corresponding distribution of simulated signal events for eleven different values of the resonance mass m_{χ} from 1.0 to 4.5 TeV. Such a model neglects the mild correlation between m_{WV} and m_{jet} , which results in a small rotation in the 2D m_{WV} and m_{jet} plane that is negligible compared to the experimental resolution uncertainties. Since the modeling of the lepton momentum scale and resolution has negligible impact in the shape of the invariant mass of the system compared to the impact of jet and $p_{\text{T}}^{\text{miss}}$ reconstruction, the electron and muon channels are merged to gain statistics for the fit in the simulation. In LP categories, an exponential function is added to the fit model of the m_{jet} dimension over its entire range, to model properly the low-mass tail. Each function parameter is interpolated for other values of m_{χ} using a polynomial function. Separate shape models are built for each studied signal benchmark scenario.

Figure 3 shows the projections of the 2D likelihood along the m_{WV} and m_{jet} dimensions, respectively. The m_{WV} projections are shown for the $G_{\text{bulk}} \rightarrow WW$ signal for mass hypotheses of 1.5, 2.5, and 4.5 TeV. The distributions are very similar for other spin hypotheses, production mechanisms, and decay modes. The m_{jet} projections are shown for $G_{\text{bulk}} \rightarrow WW$, $W' \rightarrow WZ$, and $W' \rightarrow WH$ signals for a mass of $m_{\chi} = 2.5$ TeV, demonstrating the sensitivity obtained by CMS reconstruction and jet substructure techniques to W , Z , and Higgs jet hypotheses. The experimental resolution for m_{jet} is found to be of the order of 10%, whereas that of m_{WV} ranges from 6% at 1 TeV to 4% at 4.5 TeV. In addition, the expected signal yield in every search category is also parameterized as a function of the collected integrated luminosity so that the resonance production cross section can later be extracted from the fit to data.

5.2 Background modeling

Background events are classified into two classes in the fit, each of which is described by a different pdf:

1. A background called $W+V/t$, for which the m_{jet} shape has two peaks, one near the W/Z boson masses and the other near the top quark mass, while m_{WV} has a falling spectrum. This resonant background is dominated by $t\bar{t}$ production, with subdominant contributions from SM diboson and single top quark production, and is defined in the simulation by requiring that both generated quarks from a hadronic V decay be located within

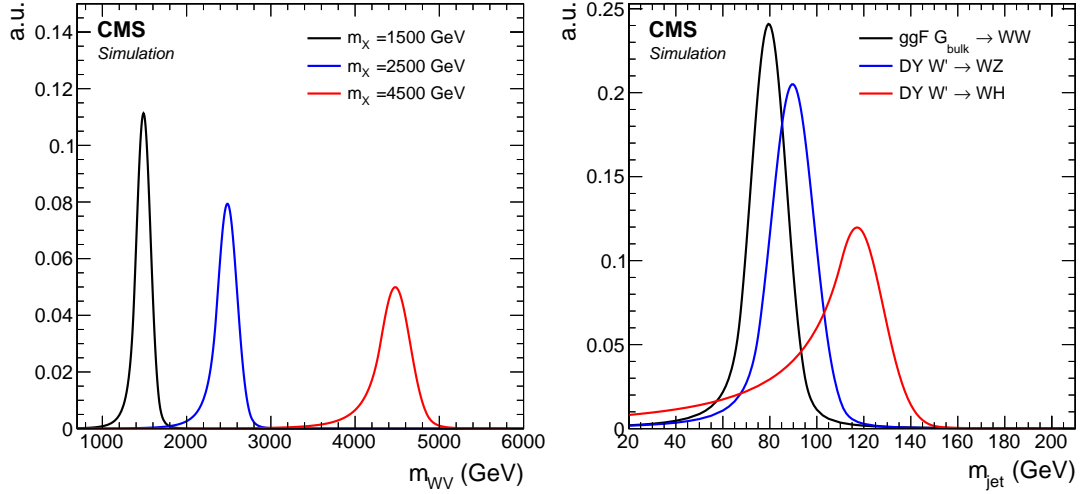


Figure 3: Projections of the 2D signal likelihood along the m_{WV} dimension (left) and the m_{jet} dimension (right). The m_{WV} projections are shown for different mass hypotheses of 1.5, 2.5, and 4.5 TeV for a G_{bulk} signal decaying to WW . The m_{jet} projections are shown for $G_{\text{bulk}} \rightarrow WW$, $W' \rightarrow WZ$, and $W' \rightarrow WH$ for $m_\chi = 2.5$ TeV. All distributions are normalized to the same area.

$\Delta R = 0.8$ of the selected large-radius jet. The m_{jet} shape structure is thus due to the selection of a partially or fully merged top quark jet or a V jet.

2. A background called W +jets, for which m_{jet} does not have a peak structure, and m_{WV} again has a falling spectrum. This nonresonant background is dominated by $W(\rightarrow \ell\nu)$ +jets events, where the selected jet is produced by the hadronization of one or more partons not originating from a vector boson but is mistagged as a V jet. In addition, this background also includes $t\bar{t}$ events where the selected merged jet corresponds to a random combination of jets in the event, instead of a W boson or top quark hadronic decay.

The W +jets and W +V/t background shapes are both described as the product of a conditional pdf of m_{WV} as a function of m_{jet} , and a m_{jet} pdf:

$$P_{W+\text{jets}}(m_{WV}, m_{\text{jet}}) = P(m_{WV}|m_{\text{jet}}, \theta) P(m_{\text{jet}}|\theta),$$

$$P_{W+V/t}(m_{WV}, m_{\text{jet}}) = P(m_{WV}|m_{\text{jet}}, \theta) P(m_{\text{jet}}|\theta),$$

where θ again represents sets of nuisance parameters, described in Section 6.1. The conditional m_{WV} pdf is constructed with a similar strategy for both classes of backgrounds that employs a robust kernel density estimation technique that is designed to provide smooth 2D templates in all subcategories. For each event in the simulated background sample, particle-level jets are clustered from stable particles using the same algorithms employed in event reconstruction. A diboson mass $m_{WV}^{\text{part.}}$ is then defined by combining the reconstructed leptonically decaying W boson and the generated large-radius jet. A detector response model is derived for the scale and resolution of the diboson mass as a function of the transverse momentum $p_{T,\text{jet}}^{\text{gen.}}$ of the generated jet, by comparing the reconstructed and generated variables m_{WV} and $m_{WV}^{\text{part.}}$. The signal region is divided into slices of the soft-drop jet mass m_{jet} : 16 slices for W +jets, and one or two slices for W +V/t in the HP and LP categories, respectively. Each simulated event i in a given m_{jet} slice then contributes to the template m_{WV} distribution in that slice by adding the following 1D

Gaussian distribution:

$$P_i(m) = \frac{w_i}{\sqrt{2\pi}\sigma(p_{T,\text{jet}}^{\text{gen.}})} \exp \left[-\frac{1}{2} \left(\frac{m - s(p_{T,\text{jet}}^{\text{gen.}}) m_{WV}^{\text{part.}}}{\sigma(p_{T,\text{jet}}^{\text{gen.}})} \right)^2 \right].$$

Here, m runs over the allowed values of m_{WV} , w_i is the event weight of the simulation, corrected for differences in the m_{WV} spectrum of W +jets observed between data and simulation in the control region, and $s(p_{T,\text{jet}}^{\text{gen.}})$ and $\sigma(p_{T,\text{jet}}^{\text{gen.}})$ are the scale and resolution parameters from the detector response model. This modified kernel procedure, seeded by the resolution instead of the event density, is robust in describing rapidly changing shapes, however it has limited performance at very low statistics. Therefore, since simulated samples do not have enough events to provide regular shapes up to the largest values of m_{WV} , these high-mass tails have to be smoothed. This smoothing is applied in the region where the event yield is dominated by Poisson statistics, namely for events with m_{WV} larger than a threshold that varies between 1.1 and 1.6 TeV depending on the background class and category. The high- m_{WV} distribution is fitted to a power-law function, which is used as the shape in this region. To improve the robustness of the templates, the electron and muon channels are here merged for the purpose of constructing the template, and in the case of W +jets, the VBF-tagged, $b\bar{b}$, and no- $b\bar{b}$ regions are merged as well. The residual differences between the 24 categories are later corrected for by the final 2D fit, deploying uncorrelated shape uncertainties that are described in Section 6.1.

The m_{jet} pdf is built separately for each of the 24 search categories, in order to account for the specific kinematic configuration of each category. For the nonresonant W +jets background, the m_{jet} pdf is obtained by smoothing the 1D histogram of selected simulated events in each category using cubic spline interpolation between bins. A kernel method, similar to the one followed for m_{WV} has limited performance in this variable since the resolution model is complex for the soft-drop mass variable. In the case of the W +V/t background, the m_{jet} distribution features a peak around the W boson mass, which is dominated by top quark jets where only the $W \rightarrow q\bar{q}'$ products were reconstructed inside the large-radius jet, and a peak around the top quark mass, where the W boson and the b quark decays are merged. To define the nominal background shapes, an analytical function is fitted to the distribution of simulated events, where the two-peak structure is modeled as the sum of two dCB functions and an exponential function that is used only in the LP categories. The inclusion of the top peak in the search region improves the fit precision, because constraining the relative fraction of the two peaks helps capture the convoluted effects of the top quark p_T spectrum and jet grooming. The m_{jet} shape of the W +V/t background in the region of the W mass peak is found to differ from that of the $X \rightarrow WW$ signals even if, in both cases, a W boson is present. This difference is attributed to the fact that the background consists of high-momentum $t\bar{t}$ events, in which a part of the b jet from the $t \rightarrow Wb$ decay overlaps with the V jet from the $W \rightarrow q\bar{q}'$ decay, while in the case of the signal, the V jet is isolated.

6 Systematic uncertainties

Systematic uncertainties affecting the normalization and shape of the signal and backgrounds are modeled by nuisance parameters, each of which is profiled in the likelihood maximization. All sources of systematic uncertainties are listed in Table 2. When specified, the magnitude of the uncertainty is the width of the function used to constrain the nuisance parameter, which is a log-normal distribution for uncertainties related to normalization, and a Gaussian distribution for parameters that control shape uncertainties. The following sections describe these

uncertainties in more detail.

Table 2: Summary of the systematic uncertainties considered in the 2D fit, the quantities they affect, and their magnitude, when applicable. When ranges are given, the magnitude of the uncertainty depends on the signal model or mass. The three parts of the table concern shape uncertainties only affecting backgrounds, shape uncertainties in the scales and resolutions, and normalization uncertainties.

Source	Relevant quantity	Magnitude
<i>Shape uncertainties only affecting backgrounds</i>		
Jet p_T spectrum	W +jets and W +V/t m_{WV} shape	
Correlation between jet mass and p_T	W +jets m_{WV} and m_{jet} shape	
Jet mass scale	W +jets m_{jet} shape	
High- m_{WV} tail	W +V/t m_{WV} shape	
W boson and top quark mass peak ratio	W +V/t m_{jet} shape	
<i>Shape uncertainties in scale and resolution</i>		
Jet mass scale	Signal and W +V/t m_{jet} mean	1%
Jet mass resolution	Signal and W +V/t m_{jet} width	8%
Jet energy scale	Signal m_{WV} mean	2%
Jet energy resolution	Signal m_{WV} width	5%
p_T^{miss} scale	Signal m_{WV} mean	2%
p_T^{miss} resolution	Signal m_{WV} width	1%
Lepton energy scale	Signal m_{WV} mean	0.5% (e), 0.3% (μ)
<i>Normalization uncertainties</i>		
W +jets normalization	W +jets yield	25%
W +V/t normalization	W +V/t yield	25%
Lepton selection efficiency	W +jets, W +V/t and signal yield	5%
V tagging	Signal yield	4% (HP), 4% (LP)
p_T -dependence of V tagging	Signal yield	1.7–19% (HP), 1.2–14% (LP)
Double-b tagging	Signal yield	6–9% ($b\bar{b}$), 0.4–2% (no- $b\bar{b}$)
$ \Delta y $ -based categorization	Signal yield	2–6% (LDy), 1.5–5.5% (HDy)
Integrated luminosity	Signal yield	1.6%
Pileup reweighting	Signal yield	1.5%
b tagging veto	Signal yield	2%
PDFs	Signal yield	0.1–2%

6.1 Systematic uncertainties in the background estimation

The 2D fit is designed to predict correctly the normalization and shapes of background contributions directly from the data by introducing nuisance parameters that vary the shapes and the yields of each contribution during the likelihood minimization process. To implement nuisance parameters that affect the shapes, the template-building procedure described in Section 5 is repeated with additional event weights or modified shape parameters. For each parameter, this produces two alternative 2D templates that represent an upward and a downward shift, between which the 2D fit performs an interpolation based on the value of the nuisance parameter. The magnitude of the shape variations are chosen to cover the differences between data and simulation observed in the control region.

First, both classes of backgrounds are assigned shape uncertainties that modify the conditional m_{WV} factor in the 2D likelihood. These have to account not only for differences between data and simulation but also for the use of common conditional likelihoods in different categories. The main difference of the shapes between the data and the templates arises from differences in the p_T spectrum after categorization and jet substructure requirements are applied. Therefore, we define alternative shapes by performing a linear reweighting of the jet p_T spectrum in each

category. This variation is motivated by the imperfect modeling of the parton distribution functions and initial-state radiation, and is conservative given that the fit has the statistical power to constrain these uncertainties in the sidebands of the 2D parameter space. The W +jets background has another shape variation related to the correlation between the jet mass and the jet p_T , which simultaneously modifies both dimensions of the conditional likelihood, while the W +V/t background is assigned an uncertainty that modifies the power-law function used to populate the high- m_{WV} tails. Since each category involves jets with different p_T spectra as a result of the selection requirements imposed on different particles in the event, these sets of nuisance parameters are left uncorrelated between categories.

Uncertainties in the m_{jet} shape of the W +jets background mostly arise from hadronization-related effects and their interplay with the soft-drop algorithm. Two m_{jet} shape variations are defined. The first one is chosen to be a simple shift of the m_{jet} scale. The second one is motivated by the study of the scaling variable $\log(m_{\text{jet}}^2/p_T)$, which reveals a difference in hadronization behavior between data and simulation. The discrepancy in the distribution of this variable is measured in the region of $m_{\text{jet}} < 50$ GeV that is dominated by W +jets events. Consequently, an uncertainty is introduced that generates alternative shapes after reweighting the simulation to match the data. Since the jet substructure variables are very sensitive to the apparent difference of the jet p_T spectrum in different categories, these uncertainties are treated as uncorrelated.

The m_{jet} shape of the W +V/t background is affected by uncertainties in the scale and resolution of the soft-drop jet mass, which are estimated by the top-enriched sample and are encoded in nuisance parameters that modify the width and the peak of the fitted dCB functions, respectively. Since the scale and resolution effects of the softdrop mass are different for two-prong and three-prong objects, these uncertainties are left uncorrelated between the W boson and top quark mass peaks and between the HP and LP categories but are considered fully correlated across other categorization criteria.

Additionally, an uncertainty of 13% in the ratio of the W boson mass peak normalization to the sum of the W boson and top quark mass peaks, derived by fitting the m_{jet} spectrum in the top-enriched control region, is introduced with one parameter per category, effectively measuring the p_T spectrum of the top quark. The shape uncertainties introduced are constrained in the fit by the shapes and relative normalizations of the W and top peaks in data.

Both the W +jets and the W +V/t backgrounds are assigned a large normalization uncertainty of 25% based on agreement between data and simulation in the low m_{jet} sideband and the top-enriched control region respectively. While the cross section measurements of these processes at the LHC are known to better precision, the effects of jet substructure, the requirement of jet mass windows, and the categorization, all introduce larger discrepancies. The motivation behind the 2D-fit signal extraction procedure is to constrain those differences from the data in each category without being sensitive to the initial value of the uncertainty. The corresponding parameters are fully correlated between lepton channels and uncorrelated across other categorization criteria and between the two background classes. Two other uncorrelated 5% background normalization parameters are assigned to the electron and muon channels in order to account for lepton triggering, reconstruction, and isolation efficiencies based on measurements from the data.

6.2 Systematic uncertainties in the signal prediction

The two-dimensional signal shapes in the (m_{jet}, m_{WV}) plane are affected by several uncertainties. Relative scale factors on the mean and width of the dCB function modeling the m_{WV} shape encode uncertainties in the scale and resolution of the jet energy and the p_T^{miss} , and electron and

muon energy scales.

In the m_{jet} dimension, two parameters account for the more important impact of grooming on the scale and resolution of the soft-drop jet mass, and are fully correlated with the analogous shape uncertainties of the W mass peak of the $W+V/t$ background.

The dominant uncertainties in the signal normalizations arise from uncertainties in the efficiency of the V tagging, double- b tagging, and $|\Delta y|$ -based selections. The corresponding nuisance parameters are anticorrelated between HP and LP, between $b\bar{b}$ and no- $b\bar{b}$, and between LDy and HDy categories, respectively, therefore inducing a migration of events between the categories in which they apply. Two nuisance parameters are associated with the τ_{21}^{DDT} -based categorization: one for its efficiency and another for its dependence on the jet p_T . The values of these nuisance parameters correspond to the statistical and systematic uncertainties of the measurement of V tagging in data for different ranges of the jet p_T . The uncertainty caused by the $|\Delta y|$ requirement is evaluated by studying the distributions of data and simulated events in the top quark-enriched control region.

Other uncertainties that apply to the normalization of signal events are associated with the integrated luminosity [73–75], the pileup reweighting, the efficiency of the b tagging veto on standard jets, and the lepton triggering, reconstruction, and isolation. Finally, uncertainties in the signal yield due to the choice of PDFs, and the factorization and renormalization scales are also taken into account: the scale uncertainties are evaluated following the proposal in Refs. [76, 77], while the PDF uncertainties are evaluated using the NNPDF 3.0 [57] PDF set. The resulting uncertainties in acceptance are found to be negligible for the scale variation and range from 0.1 to 2% for the PDF evaluation. On the other hand, the uncertainties in the signal cross section due to PDFs and scales are not taken into account in the statistical interpretation but are instead considered as uncertainties in the theoretical cross section.

7 Results

The 2D maximum likelihood fit is performed simultaneously in all 24 search categories. The results of the fit are illustrated for six representative categories in Figs. 4 and 5, where projections of the 2D post-fit distributions are shown in the m_{jet} and m_{WV} dimensions, respectively. The distributions for the remaining 18 categories show very similar levels of agreement. The jet mass distributions demonstrate good modeling of both the resonant peaks and the continuum for all categories. In the LP categories, the $W+V/t$ background has significant contributions from the W boson peak and top quark peak, while only the W peak is visible in the HP categories.

The post-fit pull distribution of the nuisance parameters is consistent with a Gaussian distribution centered around zero with a standard deviation of unity, while the best-fit values of most nuisance parameters are found to lie within the $\pm 1\sigma$ range initially associated with each uncertainty. The quality of the fit is also assessed with a goodness-of-fit estimator that uses the saturated model [78], and the observed value of the estimator falls well within the central 68% interval defined from pseudo-experiments.

No significant excess is observed over the estimated background. The largest deviation from the background hypothesis is observed for a VBF-produced charged spin-1 resonance decaying to WZ with mass around 1 TeV, with a local significance of 3.0 standard deviations.

The results are interpreted in terms of exclusion limits at 95% confidence level (CL). While the interpretation is performed for a well-defined set of benchmark signal models, the results

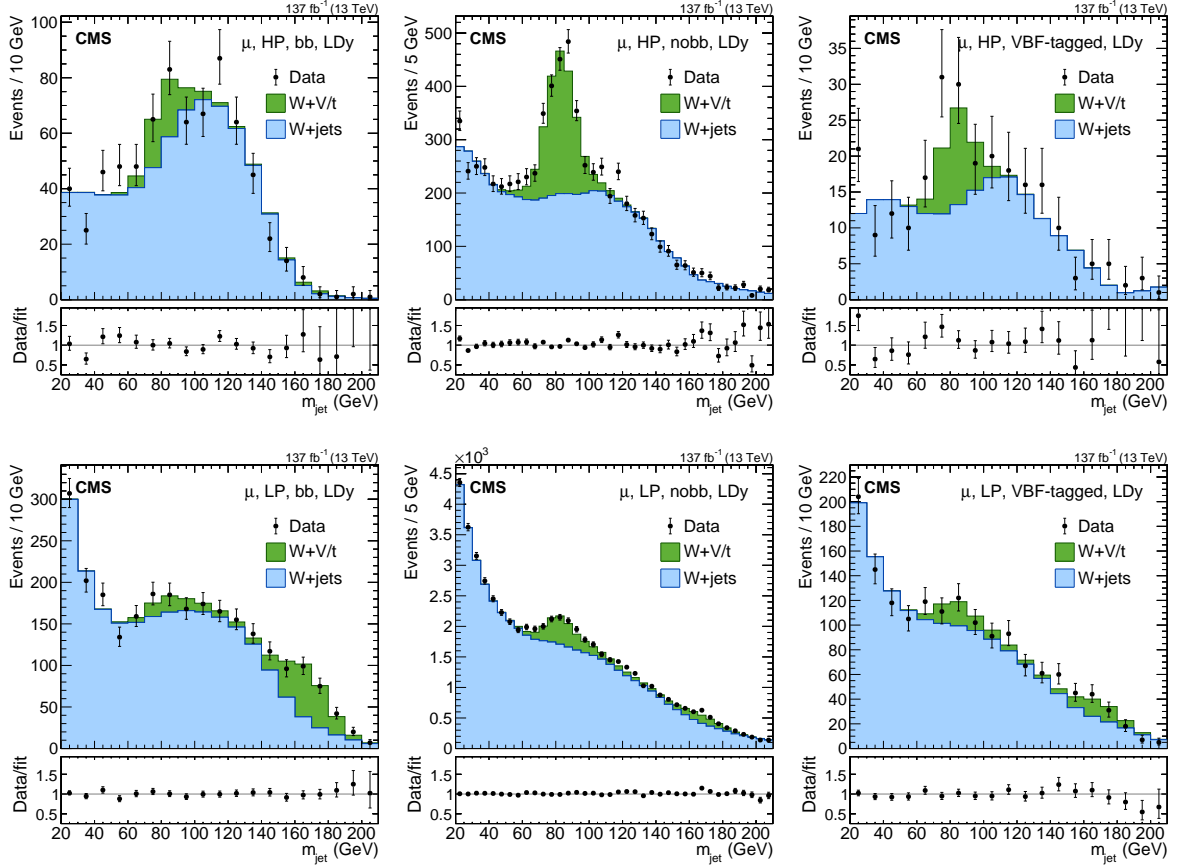


Figure 4: Comparison between the fit result and data distributions of m_{jet} in six representative muon-LDy categories. The distributions in the remaining 18 categories show very similar levels of agreement. The statistical uncertainties of the data are shown as vertical bars. The lower panels show the ratio of the data to the fit result.

are generally relevant for narrow resonances of a given spin and production mechanism. The limits are evaluated using the asymptotic approximation [79] of the CL_s method [80, 81].

Figures 6, 7, and 8 show the upper exclusion limits on the product of the resonance production cross section and the branching fraction to pairs of bosons, as functions of the resonance mass, for spin-2, spin-0, and spin-1 signal models, respectively. For ggF-produced $G_{\text{bulk}} \rightarrow WW$ resonances and for $W' \rightarrow WZ$ resonances from HVT model B, the median expected limits are more stringent than those presented in Ref. [22] by a factor of 4 to 5, benefiting from both the larger data sample, the improved analysis techniques, and the new event categories based on τ_{21}^{DDT} and $|\Delta y|$.

By comparing the observed limits to the expected cross sections from theoretical calculations, mass exclusion limits can be set for resonances produced via ggF and DY. For spin-0 resonances decaying to WW, ggF-produced bulk radions with masses below 3.1 TeV are excluded at 95% CL. For the spin-1 resonances of HVT model B, DY-produced $Z' \rightarrow WW$ resonances lighter than 4.0 TeV, $W' \rightarrow WZ$ resonances lighter than 3.9 TeV, and $W' \rightarrow WH$ resonances lighter than 4.0 TeV are excluded at 95% CL. For spin-2 resonances decaying to WW, ggF-produced bulk gravitons with masses below 1.8 TeV are excluded at 95% CL. For resonances produced only via VBF, the present data do not yet have sensitivity to exclude resonance masses for the benchmark scenarios and mass range under study.

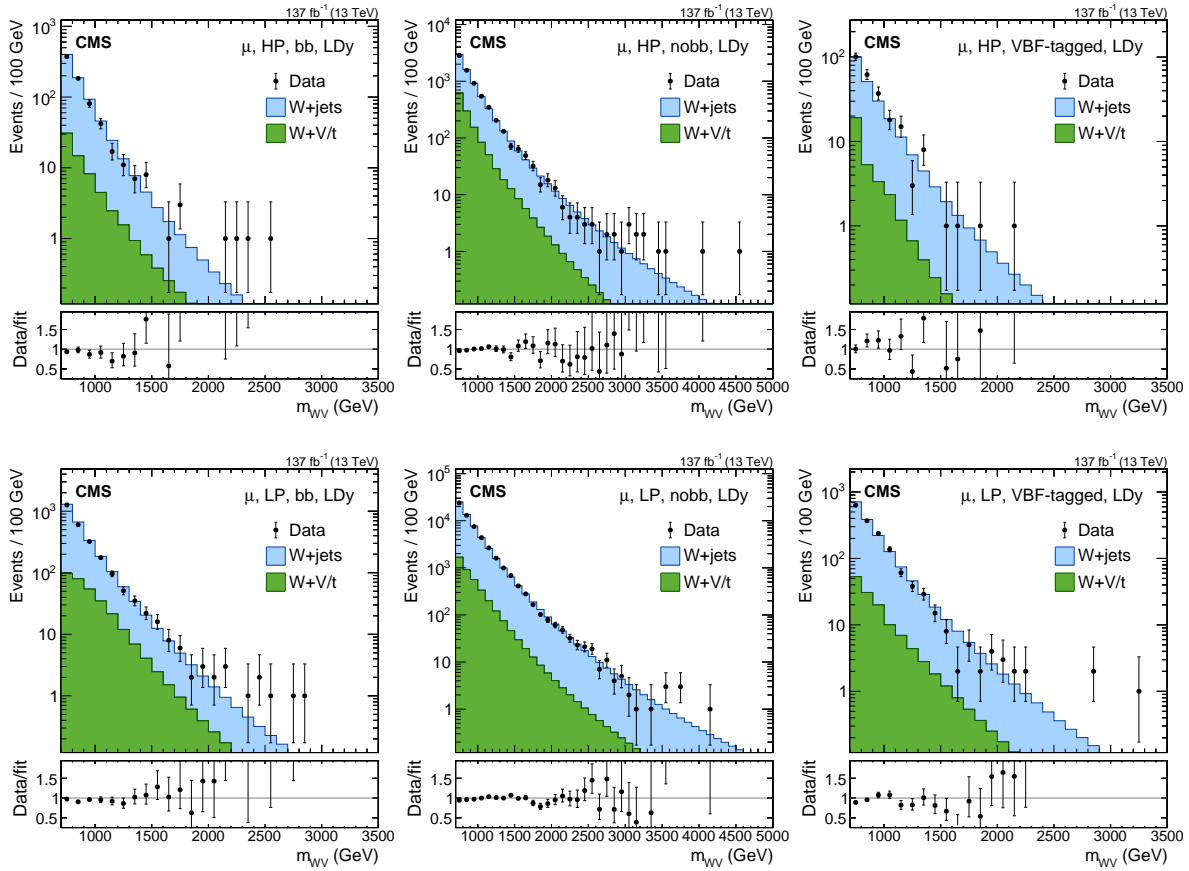


Figure 5: Comparison between the fit result and data distributions of m_{WW} in six representative muon-LDy categories. The distributions in the remaining 18 categories show very similar levels of agreement. The statistical uncertainties of the data are shown as vertical bars. The lower panels show the ratio of the data to the fit result.

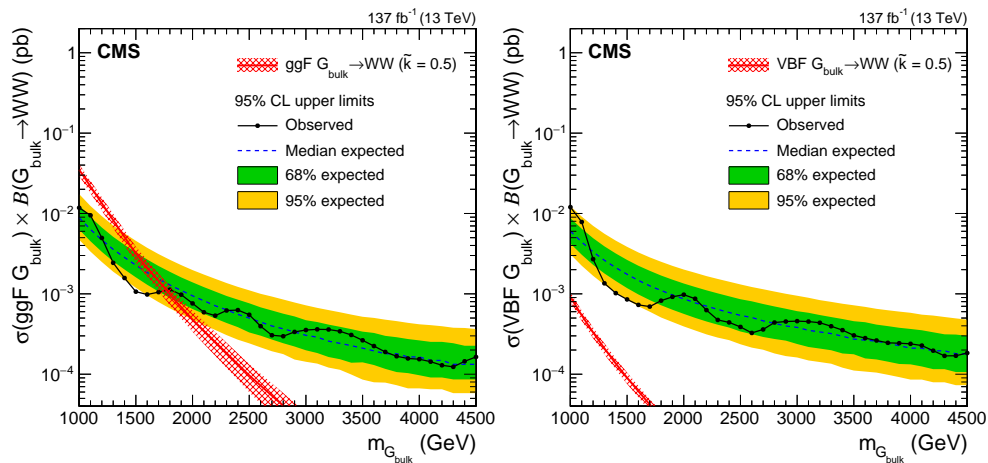


Figure 6: Exclusion limits on the product of the production cross section and the branching fraction for a new spin-2 resonance produced via gluon-gluon fusion (left) or vector boson fusion (right) and decaying to WW , as functions of the resonance mass hypothesis, compared with the predicted cross sections for a spin-2 bulk graviton with $\tilde{k} = 0.5$. Signal cross section uncertainties are shown as red cross-hatched bands.

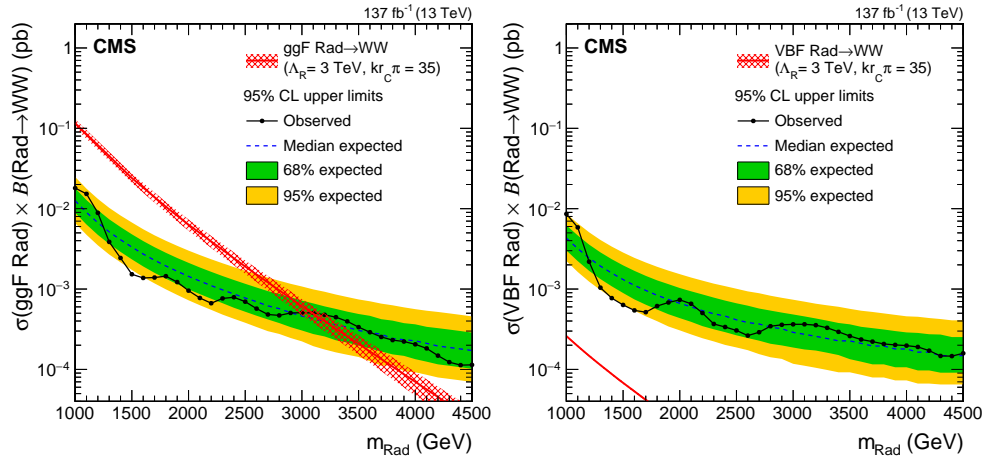


Figure 7: Exclusion limits on the product of the production cross section and the branching fraction for a new spin-0 resonance produced via gluon-gluon fusion (left) or vector boson fusion (right) and decaying to WW, as functions of the resonance mass hypothesis, compared with the predicted cross sections for a spin-0 bulk radion with $\Lambda_R = 3 \text{ TeV}$ and $kr_c \pi = 35$. Signal cross section uncertainties are shown as red cross-hatched bands.

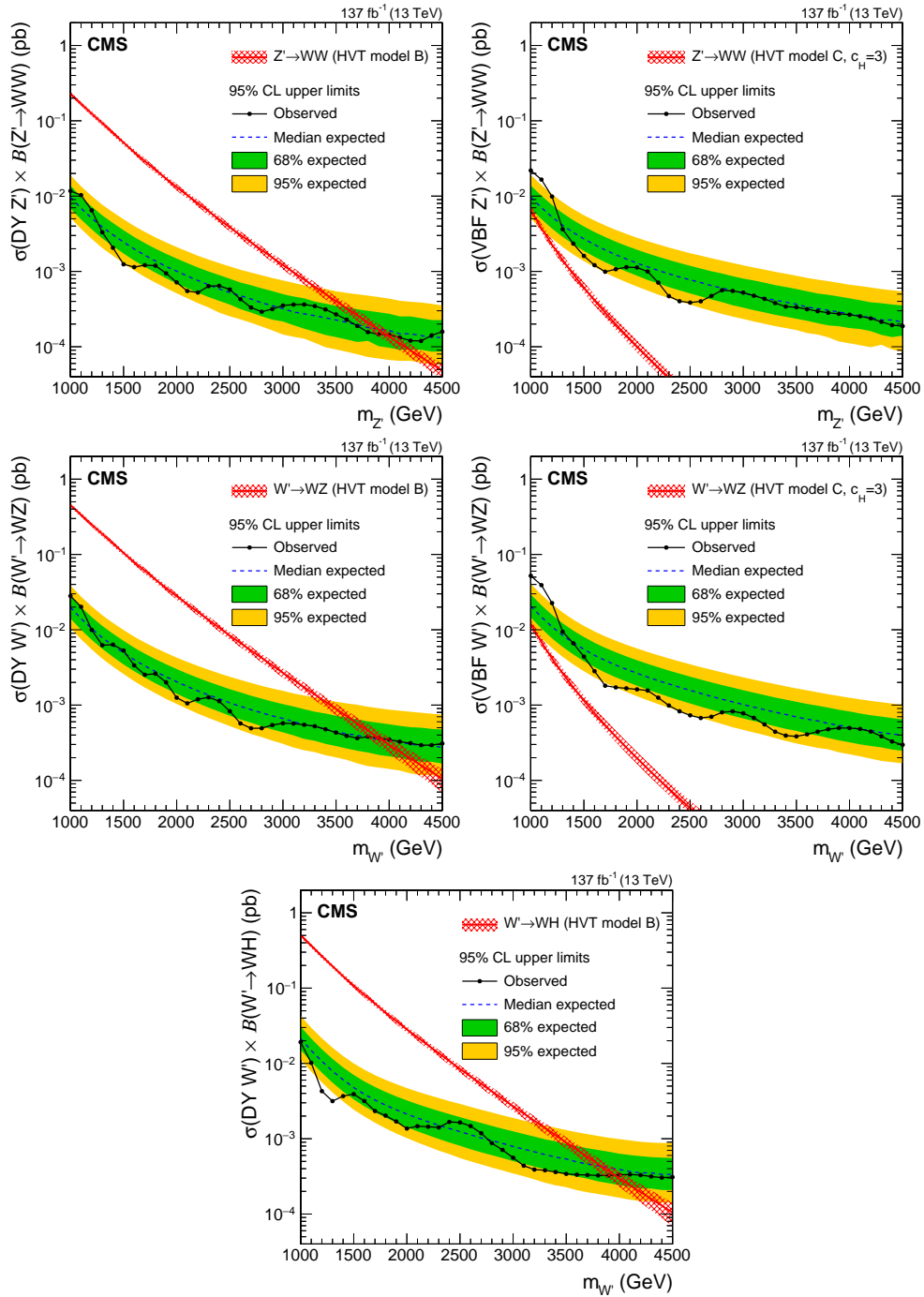


Figure 8: Exclusion limits on the product of the production cross section and the branching fraction for a new neutral spin-1 resonance produced via $q\bar{q}$ annihilation (upper left) or vector boson fusion (upper right) and decaying to WW , for a new charged spin-1 resonance produced via $q\bar{q}$ annihilation (center left) or vector boson fusion (center right) and decaying to WZ , and for a new charged spin-1 resonance produced via $q\bar{q}$ annihilation and decaying to WH (lower), as functions of the resonance mass hypothesis, compared with the predicted cross sections for a W' or Z' from HVT model B (for DY) or HVT model C with $c_H = 3$ (for VBF). Signal cross section uncertainties are shown as red cross-hatched bands.

8 Summary

A search for new narrow heavy resonances with mass larger than 1 TeV and decaying to WW , WZ , or WH boson pairs is performed using proton-proton collision events at $\sqrt{s} = 13$ TeV containing one high- p_T electron or muon, large missing transverse momentum, and a massive large-radius jet. The data were collected with the CMS detector at the LHC in 2016–2018 and correspond to an integrated luminosity of 137 fb^{-1} . The signal extraction strategy is structured around a two-dimensional maximum-likelihood fit to the distributions of the diboson reconstructed mass and the soft-drop jet mass. The sensitivity to different final states and production mechanisms is enhanced by the use of event categories that exploit the mass-decorrelated N -subjettiness ratio, the double- b tagger, the presence of a pair of forward jets compatible with vector boson fusion production, and the difference in rapidity between the reconstructed bosons. No significant excess is found, and the results are interpreted in terms of upper limits on the production cross section of new narrow resonances in several benchmark models. Spin-2 ggF-produced bulk gravitons with masses below 1.8 TeV and decaying to WW are excluded at 95% CL. Spin-1 DY-produced $Z' \rightarrow WW$ resonances lighter than 4.0 TeV, $W' \rightarrow WZ$ resonances lighter than 3.9 TeV, and $W' \rightarrow WH$ resonances lighter than 4.0 TeV in the context of HVT model B are excluded at 95% CL. Spin-0 ggF-produced bulk radions with masses below 3.1 TeV, decaying to WW , are excluded at 95% CL. Finally, for particles produced exclusively by vector boson fusion, the present data do not yet have sensitivity to exclude the benchmark scenarios under study. The reported limits, also provided in tabulated form in the HEPData record [82] for this analysis, are generally relevant for any narrow heavy resonance with a given spin produced by gluon fusion, $q\bar{q}$ annihilation, or vector boson fusion. The excluded cross section values set the most stringent experimental bounds to date.

Acknowledgments

We congratulate our colleagues in the CERN accelerator departments for the excellent performance of the LHC and thank the technical and administrative staffs at CERN and at other CMS institutes for their contributions to the success of the CMS effort. In addition, we gratefully acknowledge the computing centers and personnel of the Worldwide LHC Computing Grid and other centers for delivering so effectively the computing infrastructure essential to our analyses. Finally, we acknowledge the enduring support for the construction and operation of the LHC, the CMS detector, and the supporting computing infrastructure provided by the following funding agencies: BMBWF and FWF (Austria); FNRS and FWO (Belgium); CNPq, CAPES, FAPERJ, FAPERGS, and FAPESP (Brazil); MES and BNSF (Bulgaria); CERN; CAS, MoST, and NSFC (China); MINCIENCIAS (Colombia); MSES and CSF (Croatia); RIF (Cyprus); SENESCYT (Ecuador); MoER, ERC PUT and ERDF (Estonia); Academy of Finland, MEC, and HIP (Finland); CEA and CNRS/IN2P3 (France); BMBF, DFG, and HGF (Germany); GSRI (Greece); NKFI (Hungary); DAE and DST (India); IPM (Iran); SFI (Ireland); INFN (Italy); MSIP and NRF (Republic of Korea); MES (Latvia); LAS (Lithuania); MOE and UM (Malaysia); BUAP, CINVESTAV, CONACYT, LNS, SEP, and UASLP-FAI (Mexico); MOS (Montenegro); MBIE (New Zealand); PAEC (Pakistan); MSHE and NSC (Poland); FCT (Portugal); JINR (Dubna); MON, RosAtom, RAS, RFBR, and NRC KI (Russia); MESTD (Serbia); SEIDI, CPAN, PCTI, and FEDER (Spain); MOSTR (Sri Lanka); Swiss Funding Agencies (Switzerland); MST (Taipei); ThEPCenter, IPST, STAR, and NSTDA (Thailand); TUBITAK and TAEK (Turkey); NASU (Ukraine); STFC (United Kingdom); DOE and NSF (USA).

Individuals have received support from the Marie-Curie program and the European Research Council and Horizon 2020 Grant, contract Nos. 675440, 724704, 752730, 758316, 765710,

824093, 884104, and COST Action CA16108 (European Union); the Leventis Foundation; the Alfred P. Sloan Foundation; the Alexander von Humboldt Foundation; the Belgian Federal Science Policy Office; the Fonds pour la Formation à la Recherche dans l'Industrie et dans l'Agriculture (FRIA-Belgium); the Agentschap voor Innovatie door Wetenschap en Technologie (IWT-Belgium); the F.R.S.-FNRS and FWO (Belgium) under the "Excellence of Science – EOS" – be.h project n. 30820817; the Beijing Municipal Science & Technology Commission, No. Z191100007219010; the Ministry of Education, Youth and Sports (MEYS) of the Czech Republic; the Deutsche Forschungsgemeinschaft (DFG), under Germany's Excellence Strategy – EXC 2121 "Quantum Universe" – 390833306, and under project number 400140256 - GRK2497; the Lendület ("Momentum") Program and the János Bolyai Research Scholarship of the Hungarian Academy of Sciences, the New National Excellence Program ÚNKP, the NK-FIA research grants 123842, 123959, 124845, 124850, 125105, 128713, 128786, and 129058 (Hungary); the Council of Science and Industrial Research, India; the Latvian Council of Science; the Ministry of Science and Higher Education and the National Science Center, contracts Opus 2014/15/B/ST2/03998 and 2015/19/B/ST2/02861 (Poland); the Fundação para a Ciência e a Tecnologia, grant CEECIND/01334/2018 (Portugal); the National Priorities Research Program by Qatar National Research Fund; the Ministry of Science and Higher Education, project no. 14.W03.31.0026 (Russia); the Programa Estatal de Fomento de la Investigación Científica y Técnica de Excelencia María de Maeztu, grant MDM-2015-0509 and the Programa Severo Ochoa del Principado de Asturias; the Stavros Niarchos Foundation (Greece); the Rachadapisek Sompot Fund for Postdoctoral Fellowship, Chulalongkorn University and the Chulalongkorn Academic into Its 2nd Century Project Advancement Project (Thailand); the Kavli Foundation; the Nvidia Corporation; the SuperMicro Corporation; the Welch Foundation, contract C-1845; and the Weston Havens Foundation (USA).

References

- [1] S. L. Glashow, "Partial symmetries of weak interactions", *Nucl. Phys.* **22** (1961) 579, doi:10.1016/0029-5582(61)90469-2.
- [2] A. Salam and J. C. Ward, "Electromagnetic and weak interactions", *Phys. Lett.* **13** (1964) 168, doi:10.1016/0031-9163(64)90711-5.
- [3] S. Weinberg, "A model of leptons", *Phys. Rev. Lett.* **19** (1967) 1264, doi:10.1103/PhysRevLett.19.1264.
- [4] ATLAS Collaboration, "Observation of a new particle in the search for the standard model Higgs boson with the ATLAS detector at the LHC", *Phys. Lett. B* **716** (2012) 1, doi:10.1016/j.physletb.2012.08.020, arXiv:1207.7214.
- [5] CMS Collaboration, "Observation of a new boson at a mass of 125 GeV with the CMS experiment at the LHC", *Phys. Lett. B* **716** (2012) 30, doi:10.1016/j.physletb.2012.08.021, arXiv:1207.7235.
- [6] CMS Collaboration, "Observation of a new boson with mass near 125 GeV in pp collisions at $\sqrt{s} = 7$ and 8 TeV", *JHEP* **06** (2013) 081, doi:10.1007/JHEP06(2013)081, arXiv:1303.4571.
- [7] L. Randall and R. Sundrum, "A large mass hierarchy from a small extra dimension", *Phys. Rev. Lett.* **83** (1999) 3370, doi:10.1103/PhysRevLett.83.3370, arXiv:hep-ph/9905221.

-
- [8] L. Randall and R. Sundrum, “An alternative to compactification”, *Phys. Rev. Lett.* **83** (1999) 4690, doi:10.1103/PhysRevLett.83.4690, arXiv:hep-th/9906064.
- [9] D. Pappadopulo, A. Thamm, R. Torre, and A. Wulzer, “Heavy vector triplets: Bridging theory and data”, *JHEP* **09** (2014) 060, doi:10.1007/JHEP09(2014)060, arXiv:1402.4431.
- [10] B. Bellazzini, C. Csáki, and J. Serra, “Composite Higgses”, *Eur. Phys. J. C* **74** (2014) 2766, doi:10.1140/epjc/s10052-014-2766-x, arXiv:1401.2457.
- [11] R. Contino, D. Marzocca, D. Pappadopulo, and R. Rattazzi, “On the effect of resonances in composite Higgs phenomenology”, *JHEP* **10** (2011) 081, doi:10.1007/JHEP10(2011)081, arXiv:1109.1570.
- [12] D. Marzocca, M. Serone, and J. Shu, “General composite Higgs models”, *JHEP* **08** (2012) 013, doi:10.1007/JHEP08(2012)013, arXiv:1205.0770.
- [13] D. Greco and D. Liu, “Hunting composite vector resonances at the LHC: naturalness facing data”, *JHEP* **12** (2014) 126, doi:10.1007/JHEP12(2014)126, arXiv:1410.2883.
- [14] K. Lane and L. Pritchett, “The light composite Higgs boson in strong extended technicolor”, *JHEP* **06** (2017) 140, doi:10.1007/JHEP06(2017)140, arXiv:1604.07085.
- [15] M. Schmaltz and D. Tucker-Smith, “Little Higgs review”, *Ann. Rev. Nucl. Part. Sci.* **55** (2005) 229, doi:10.1146/annurev.nucl.55.090704.151502, arXiv:hep-ph/0502182.
- [16] N. Arkani-Hamed, A. G. Cohen, E. Katz, and A. E. Nelson, “The littlest Higgs”, *JHEP* **07** (2002) 034, doi:10.1088/1126-6708/2002/07/034, arXiv:hep-ph/0206021.
- [17] ATLAS Collaboration, “Search for production of WW/WZ resonances decaying to a lepton, neutrino and jets in pp collisions at $\sqrt{s} = 8$ TeV with the ATLAS detector”, *Eur. Phys. J. C* **75** (2015) 209, doi:10.1140/epjc/s10052-015-3425-6, arXiv:1503.04677. [Erratum: doi:10.1140/epjc/s10052-015-3593-4].
- [18] ATLAS Collaboration, “Searches for heavy diboson resonances in pp collisions at $\sqrt{s} = 13$ TeV with the ATLAS detector”, *JHEP* **09** (2016) 173, doi:10.1007/JHEP09(2016)173, arXiv:1606.04833.
- [19] ATLAS Collaboration, “Search for WW/WZ resonance production in $\ell\nu qq$ final states in pp collisions at $\sqrt{s} = 13$ TeV with the ATLAS detector”, *JHEP* **03** (2018) 042, doi:10.1007/JHEP03(2018)042, arXiv:1710.07235.
- [20] CMS Collaboration, “Search for massive resonances decaying into pairs of boosted bosons in semi-leptonic final states at $\sqrt{s} = 8$ TeV”, *JHEP* **08** (2014) 174, doi:10.1007/JHEP08(2014)174, arXiv:1405.3447.
- [21] CMS Collaboration, “Search for massive resonances decaying into WW, WZ or ZZ bosons in proton-proton collisions at $\sqrt{s} = 13$ TeV”, *JHEP* **03** (2017) 162, doi:10.1007/JHEP03(2017)162, arXiv:1612.09159.

- [22] CMS Collaboration, “Search for a heavy resonance decaying to a pair of vector bosons in the lepton plus merged jet final state at $\sqrt{s} = 13$ TeV”, *JHEP* **05** (2018) 088, doi:10.1007/JHEP05(2018)088, arXiv:1802.09407.
- [23] ATLAS Collaboration, “Search for heavy diboson resonances in semileptonic final states in pp collisions at $\sqrt{s} = 13$ TeV with the ATLAS detector”, *Eur. Phys. J. C* **80** (2020), no. 12, 1165, doi:10.1140/epjc/s10052-020-08554-y, arXiv:2004.14636.
- [24] ATLAS Collaboration, “Search for a new resonance decaying to a W or Z boson and a Higgs boson in the $\ell\ell/\ell\nu/\nu\nu + b\bar{b}$ final states with the ATLAS detector”, *Eur. Phys. J. C* **75** (2015) 263, doi:10.1140/epjc/s10052-015-3474-x, arXiv:1503.08089.
- [25] ATLAS Collaboration, “Search for new resonances decaying to a W or Z boson and a Higgs boson in the $\ell^+\ell^-\bar{b}\bar{b}$, $\ell\nu b\bar{b}$, and $\nu\bar{\nu}b\bar{b}$ channels with pp collisions at $\sqrt{s} = 13$ TeV with the ATLAS detector”, *Phys. Lett. B* **765** (2017) 32, doi:10.1016/j.physletb.2016.11.045, arXiv:1607.05621.
- [26] ATLAS Collaboration, “Search for heavy resonances decaying into a W or Z boson and a Higgs boson in final states with leptons and b-jets in 36 fb^{-1} of $\sqrt{s} = 13$ TeV pp collisions with the ATLAS detector”, *JHEP* **03** (2018) 174, doi:10.1007/JHEP03(2018)174, arXiv:1712.06518.
- [27] CMS Collaboration, “Search for massive WH resonances decaying into the $\ell\nu b\bar{b}$ final state at $\sqrt{s} = 8$ TeV”, *Eur. Phys. J. C* **76** (2016) 237, doi:10.1140/epjc/s10052-016-4067-z, arXiv:1601.06431.
- [28] CMS Collaboration, “Search for heavy resonances decaying into a vector boson and a Higgs boson in final states with charged leptons, neutrinos, and b quarks”, *Phys. Lett. B* **768** (2017) 137, doi:10.1016/j.physletb.2017.02.040, arXiv:1610.08066.
- [29] CMS Collaboration, “Search for heavy resonances decaying into a vector boson and a Higgs boson in final states with charged leptons, neutrinos and b quarks at $\sqrt{s} = 13$ TeV”, *JHEP* **11** (2018) 172, doi:10.1007/JHEP11(2018)172, arXiv:1807.02826.
- [30] CMS Collaboration, “The CMS experiment at the CERN LHC”, *JINST* **3** (2008) S08004, doi:10.1088/1748-0221/3/08/S08004.
- [31] CMS Collaboration, “Particle-flow reconstruction and global event description with the CMS detector”, *JINST* **12** (2017) P10003, doi:10.1088/1748-0221/12/10/P10003, arXiv:1706.04965.
- [32] CMS Collaboration, “Performance of missing transverse momentum reconstruction in proton-proton collisions at $\sqrt{s} = 13$ TeV using the CMS detector”, *JINST* **14** (2019) P07004, doi:10.1088/1748-0221/14/07/P07004, arXiv:1903.06078.
- [33] M. Cacciari, G. P. Salam, and G. Soyez, “The anti- k_T jet clustering algorithm”, *JHEP* **04** (2008) 063, doi:10.1088/1126-6708/2008/04/063, arXiv:0802.1189.
- [34] M. Cacciari, G. P. Salam, and G. Soyez, “FastJet user manual”, *Eur. Phys. J. C* **72** (2012) 1896, doi:10.1140/epjc/s10052-012-1896-2, arXiv:1111.6097.
- [35] CMS Collaboration, “Jet energy scale and resolution in the CMS experiment in pp collisions at 8 TeV”, *JINST* **12** (2017) P02014, doi:10.1088/1748-0221/12/02/P02014, arXiv:1607.03663.

-
- [36] CMS Collaboration, “Pileup mitigation at CMS in 13 TeV data”, *JINST* **15** (2020) P09018, doi:10.1088/1748-0221/15/09/p09018, arXiv:2003.00503.
- [37] D. Bertolini, P. Harris, M. Low, and N. Tran, “Pileup per particle identification”, *JHEP* **10** (2014) 059, doi:10.1007/JHEP10(2014)059, arXiv:1407.6013.
- [38] CMS Collaboration, “Performance of the CMS Level-1 trigger in proton-proton collisions at $\sqrt{s} = 13$ TeV”, *JINST* **15** (2020) P10017, doi:10.1088/1748-0221/15/10/P10017, arXiv:2006.10165.
- [39] CMS Collaboration, “The CMS trigger system”, *JINST* **12** (2017) P01020, doi:10.1088/1748-0221/12/01/P01020, arXiv:1609.02366.
- [40] W. D. Goldberger and M. B. Wise, “Modulus stabilization with bulk fields”, *Phys. Rev. Lett.* **83** (1999) 4922, doi:10.1103/PhysRevLett.83.4922, arXiv:hep-ph/9907447.
- [41] C. Csaki, M. Graesser, L. Randall, and J. Terning, “Cosmology of brane models with radion stabilization”, *Phys. Rev. D* **62** (2000) 045015, doi:10.1103/PhysRevD.62.045015, arXiv:hep-ph/9911406.
- [42] C. Csaki, M. L. Graesser, and G. D. Kribs, “Radion dynamics and electroweak physics”, *Phys. Rev. D* **63** (2001) 065002, doi:10.1103/PhysRevD.63.065002, arXiv:hep-th/0008151.
- [43] K. Agashe, H. Davoudiasl, G. Perez, and A. Soni, “Warped gravitons at the LHC and beyond”, *Phys. Rev. D* **76** (2007) 036006, doi:10.1103/PhysRevD.76.036006, arXiv:hep-ph/0701186.
- [44] A. L. Fitzpatrick, J. Kaplan, L. Randall, and L.-T. Wang, “Searching for the Kaluza-Klein graviton in bulk RS models”, *JHEP* **09** (2007) 013, doi:10.1088/1126-6708/2007/09/013, arXiv:hep-ph/0701150.
- [45] O. Antipin, D. Atwood, and A. Soni, “Search for RS gravitons via $W_L W_L$ decays”, *Phys. Lett. B* **666** (2008) 155, doi:10.1016/j.physletb.2008.07.009, arXiv:0711.3175.
- [46] A. Oliveira, “Gravity particles from warped extra dimensions, predictions for LHC”, 2014. arXiv:1404.0102.
- [47] J. Alwall et al., “The automated computation of tree-level and next-to-leading order differential cross sections, and their matching to parton shower simulations”, *JHEP* **07** (2014) 079, doi:10.1007/JHEP07(2014)079, arXiv:1405.0301.
- [48] P. Nason, “A new method for combining NLO QCD with shower Monte Carlo algorithms”, *JHEP* **11** (2004) 040, doi:10.1088/1126-6708/2004/11/040, arXiv:hep-ph/0409146.
- [49] S. Frixione, P. Nason, and C. Oleari, “Matching NLO QCD computations with parton shower simulations: the POWHEG method”, *JHEP* **11** (2007) 070, doi:10.1088/1126-6708/2007/11/070, arXiv:0709.2092.
- [50] S. Alioli, P. Nason, C. Oleari, and E. Re, “A general framework for implementing NLO calculations in shower Monte Carlo programs: the POWHEG BOX”, *JHEP* **06** (2010) 043, doi:10.1007/JHEP06(2010)043, arXiv:1002.2581.

- [51] S. Alioli, S.-O. Moch, and P. Uwer, “Hadronic top-quark pair-production with one jet and parton showering”, *JHEP* **01** (2012) 137, doi:10.1007/JHEP01(2012)137, arXiv:1110.5251.
- [52] S. Alioli, P. Nason, C. Oleari, and E. Re, “NLO single-top production matched with shower in POWHEG: s - and t -channel contributions”, *JHEP* **09** (2009) 111, doi:10.1007/JHEP02(2010)011, arXiv:0907.4076. [Erratum: doi:10.1088/1126-6708/2009/09/111].
- [53] E. Re, “Single-top Wt -channel production matched with parton showers using the POWHEG method”, *Eur. Phys. J. C* **71** (2011) 1547, doi:10.1140/epjc/s10052-011-1547-z, arXiv:1009.2450.
- [54] R. Frederix and S. Frixione, “Merging meets matching in MC@NLO”, *JHEP* **12** (2012) 061, doi:10.1007/JHEP12(2012)061, arXiv:1209.6215.
- [55] P. Nason and G. Zanderighi, “ W^+W^- , WZ and ZZ production in the POWHEG-BOX-V2”, *Eur. Phys. J. C* **74** (2014) 2702, doi:10.1140/epjc/s10052-013-2702-5, arXiv:1311.1365.
- [56] T. Sjöstrand et al., “An introduction to PYTHIA 8.2”, *Comput. Phys. Commun.* **191** (2015) 159, doi:10.1016/j.cpc.2015.01.024, arXiv:1410.3012.
- [57] NNPDF Collaboration, “Parton distributions for the LHC Run II”, *JHEP* **04** (2015) 040, doi:10.1007/JHEP04(2015)040, arXiv:1410.8849.
- [58] CMS Collaboration, “Event generator tunes obtained from underlying event and multiparton scattering measurements”, *Eur. Phys. J. C* **76** (2016) 155, doi:10.1140/epjc/s10052-016-3988-x, arXiv:1512.00815.
- [59] CMS Collaboration, “Investigations of the impact of the parton shower tuning in Pythia 8 in the modelling of $t\bar{t}$ at $\sqrt{s} = 8$ and 13 TeV”, CMS Physics Analysis Summary CMS-PAS-TOP-16-021, 2016.
- [60] NNPDF Collaboration, “Parton distributions from high-precision collider data”, *Eur. Phys. J. C* **77** (2017) 663, doi:10.1140/epjc/s10052-017-5199-5, arXiv:1706.00428.
- [61] CMS Collaboration, “Extraction and validation of a new set of CMS PYTHIA8 tunes from underlying-event measurements”, *Eur. Phys. J. C* **80** (2020) 4, doi:10.1140/epjc/s10052-019-7499-4, arXiv:1903.12179.
- [62] GEANT4 Collaboration, “GEANT4 — a simulation toolkit”, *Nucl. Instrum. Meth. A* **506** (2003) 250, doi:10.1016/S0168-9002(03)01368-8.
- [63] CMS Collaboration, “Electron and photon reconstruction and identification with the CMS experiment at the CERN LHC”, *JINST* **16** (2021) P05014, doi:10.1088/1748-0221/16/05/P05014, arXiv:2012.06888.
- [64] CMS Collaboration, “Performance of the reconstruction and identification of high-momentum muons in proton-proton collisions at $\sqrt{s} = 13$ TeV”, *JINST* **15** (2020) P02027, doi:10.1088/1748-0221/15/02/P02027, arXiv:1912.03516.
- [65] CMS Collaboration, “Jet algorithms performance in 13 TeV data”, CMS Physics Analysis Summary CMS-PAS-JME-16-003, 2017.

-
- [66] M. Dasgupta, A. Fregoso, S. Marzani, and G. P. Salam, “Towards an understanding of jet substructure”, *JHEP* **09** (2013) 029, doi:10.1007/JHEP09(2013)029, arXiv:1307.0007.
- [67] J. M. Butterworth, A. R. Davison, M. Rubin, and G. P. Salam, “Jet substructure as a new Higgs search channel at the LHC”, *Phys. Rev. Lett.* **100** (2008) 242001, doi:10.1103/PhysRevLett.100.242001, arXiv:0802.2470.
- [68] A. J. Larkoski, S. Marzani, G. Soyez, and J. Thaler, “Soft drop”, *JHEP* **05** (2014) 146, doi:10.1007/JHEP05(2014)146, arXiv:1402.2657.
- [69] J. Thaler and K. Van Tilburg, “Identifying boosted objects with N -subjettiness”, *JHEP* **03** (2011) 015, doi:10.1007/JHEP03(2011)015, arXiv:1011.2268.
- [70] J. Dolen et al., “Thinking outside the ROCs: Designing decorrelated taggers (DDT) for jet substructure”, *JHEP* **05** (2016) 156, doi:10.1007/JHEP05(2016)156, arXiv:1603.00027.
- [71] CMS Collaboration, “Identification of heavy-flavour jets with the CMS detector in pp collisions at 13 TeV”, *JINST* **13** (2018) P05011, doi:10.1088/1748-0221/13/05/P05011, arXiv:1712.07158.
- [72] M. J. Oreglia, “A study of the reactions $\psi' \rightarrow \gamma\gamma\psi$ ”. PhD thesis, Stanford University, 1980. SLAC Report SLAC-R-236.
- [73] CMS Collaboration, “Precision luminosity measurement in proton-proton collisions at $\sqrt{s} = 13$ TeV in 2015 and 2016 at CMS”, 2021. arXiv:2104.01927. Accepted by *Eur. Phys. J. C*.
- [74] CMS Collaboration, “CMS luminosity measurement for the 2017 data-taking period at $\sqrt{s} = 13$ TeV”, CMS Physics Analysis Summary CMS-PAS-LUM-17-004, 2018.
- [75] CMS Collaboration, “CMS luminosity measurement for the 2018 data-taking period at $\sqrt{s} = 13$ TeV”, CMS Physics Analysis Summary CMS-PAS-LUM-18-002, 2019.
- [76] M. Cacciari et al., “The $t\bar{t}$ cross-section at 1.8 TeV and 1.96 TeV: A study of the systematics due to parton densities and scale dependence”, *JHEP* **04** (2004) 068, doi:10.1088/1126-6708/2004/04/068, arXiv:hep-ph/0303085.
- [77] S. Catani, D. de Florian, M. Grazzini, and P. Nason, “Soft gluon resummation for Higgs boson production at hadron colliders”, *JHEP* **07** (2003) 028, doi:10.1088/1126-6708/2003/07/028, arXiv:hep-ph/0306211.
- [78] S. Baker and R. D. Cousins, “Clarification of the use of chi square and likelihood functions in fits to histograms”, *Nucl. Instrum. Meth.* **221** (1984) 437, doi:10.1016/0167-5087(84)90016-4.
- [79] G. Cowan, K. Cranmer, E. Gross, and O. Vitells, “Asymptotic formulae for likelihood-based tests of new physics”, *Eur. Phys. J. C* **71** (2011) 1554, doi:10.1140/epjc/s10052-011-1554-0, arXiv:1007.1727. [Erratum: doi:10.1140/epjc/s10052-013-2501-z].
- [80] T. Junk, “Confidence level computation for combining searches with small statistics”, *Nucl. Instrum. Meth. A* **434** (1999) 435, doi:10.1016/S0168-9002(99)00498-2, arXiv:hep-ex/9902006.

-
- [81] A. L. Read, "Presentation of search results: The CL_s technique", *J. Phys. G* **28** (2002) 2693, doi:10.1088/0954-3899/28/10/313.
- [82] "HEPData record for this analysis", 2021. doi:10.17182/hepdata.102465.

A The CMS Collaboration

Yerevan Physics Institute, Yerevan, Armenia

A. Tumasyan

Institut für Hochenergiephysik, Vienna, Austria

W. Adam, J.W. Andrejkovic, T. Bergauer, S. Chatterjee, M. Dragicevic, A. Escalante Del Valle, R. Frühwirth¹, M. Jeitler¹, N. Krammer, L. Lechner, D. Liko, I. Mikulec, P. Paulitsch, F.M. Pitters, J. Schieck¹, R. Schöfbeck, M. Spanring, S. Templ, W. Waltenberger, C.-E. Wulz¹

Institute for Nuclear Problems, Minsk, Belarus

V. Chekhovsky, A. Litomin, V. Makarenko

Universiteit Antwerpen, Antwerpen, Belgium

M.R. Darwish², E.A. De Wolf, X. Janssen, T. Kello³, A. Lelek, H. Rejeb Sfar, P. Van Mechelen, S. Van Putte, N. Van Remortel

Vrije Universiteit Brussel, Brussel, Belgium

F. Blekman, E.S. Bols, J. D'Hondt, J. De Clercq, M. Delcourt, H. El Faham, S. Lowette, S. Moortgat, A. Morton, D. Müller, A.R. Sahasransu, S. Tavernier, W. Van Doninck, P. Van Mulders

Université Libre de Bruxelles, Bruxelles, Belgium

D. Beghin, B. Bilin, B. Clerboux, G. De Lentdecker, L. Favart, A. Grebenyuk, A.K. Kalsi, K. Lee, M. Mahdavihorrami, I. Makarenko, L. Moureaux, L. Pétré, A. Popov, N. Postiau, E. Starling, L. Thomas, M. Vanden Bemden, C. Vander Velde, P. Vanlaer, D. Vannerom, L. Wezenbeek

Ghent University, Ghent, Belgium

T. Cornelis, D. Dobur, J. Knolle, L. Lambrecht, G. Mestdach, M. Niedziela, C. Roskas, A. Samalan, K. Skovpen, M. Tytgat, W. Verbeke, B. Vermassen, M. Vit

Université Catholique de Louvain, Louvain-la-Neuve, Belgium

A. Bethani, G. Bruno, F. Bury, C. Caputo, P. David, C. Delaere, I.S. Donertas, A. Giammanco, K. Jaffel, Sa. Jain, V. Lemaitre, K. Mondal, J. Prisciandaro, A. Taliercio, M. Teklishyn, T.T. Tran, P. Vischia, S. Wertz

Centro Brasileiro de Pesquisas Fisicas, Rio de Janeiro, Brazil

G.A. Alves, C. Hensel, A. Moraes

Universidade do Estado do Rio de Janeiro, Rio de Janeiro, Brazil

W.L. Aldá Júnior, M. Alves Gallo Pereira, M. Barroso Ferreira Filho, H. BRANDAO MALBOUISSON, W. Carvalho, J. Chinellato⁴, E.M. Da Costa, G.G. Da Silveira⁵, D. De Jesus Damiao, S. Fonseca De Souza, D. Matos Figueiredo, C. Mora Herrera, K. Mota Amarilo, L. Mundim, H. Nogima, P. Rebello Teles, A. Santoro, S.M. Silva Do Amaral, A. Sznajder, M. Thiel, F. Torres Da Silva De Araujo, A. Vilela Pereira

Universidade Estadual Paulista ^a, Universidade Federal do ABC ^b, São Paulo, Brazil

C.A. Bernardes^{a,a,5}, L. Calligaris^a, T.R. Fernandez Perez Tomei^a, E.M. Gregores^{a,b}, D.S. Lemos^a, P.G. Mercadante^{a,b}, S.F. Novaes^a, Sandra S. Padula^a

Institute for Nuclear Research and Nuclear Energy, Bulgarian Academy of Sciences, Sofia, Bulgaria

A. Aleksandrov, G. Antchev, R. Hadjiiska, P. Iaydjiev, M. Misheva, M. Rodozov, M. Shopova, G. Sultanov

University of Sofia, Sofia, Bulgaria

A. Dimitrov, T. Ivanov, L. Litov, B. Pavlov, P. Petkov, A. Petrov

Beihang University, Beijing, China

T. Cheng, Q. Guo, T. Javaid⁶, M. Mittal, H. Wang, L. Yuan

Department of Physics, Tsinghua University

M. Ahmad, G. Bauer, C. Dozen⁷, Z. Hu, J. Martins⁸, Y. Wang, K. Yi^{9,10}

Institute of High Energy Physics, Beijing, China

E. Chapon, G.M. Chen⁶, H.S. Chen⁶, M. Chen, F. Iemmi, A. Kapoor, D. Leggat, H. Liao, Z.-A. LIU⁶, V. Milosevic, F. Monti, R. Sharma, J. Tao, J. Thomas-wilsker, J. Wang, H. Zhang, S. Zhang⁶, J. Zhao

State Key Laboratory of Nuclear Physics and Technology, Peking University, Beijing, China

A. Agapitos, Y. An, Y. Ban, C. Chen, A. Levin, Q. Li, X. Lyu, Y. Mao, S.J. Qian, D. Wang, Q. Wang, J. Xiao

Sun Yat-Sen University, Guangzhou, China

M. Lu, Z. You

Institute of Modern Physics and Key Laboratory of Nuclear Physics and Ion-beam Application (MOE) - Fudan University, Shanghai, China

X. Gao³, H. Okawa

Zhejiang University, Hangzhou, China

Z. Lin, M. Xiao

Universidad de Los Andes, Bogota, Colombia

C. Avila, A. Cabrera, C. Florez, J. Fraga, A. Sarkar, M.A. Segura Delgado

Universidad de Antioquia, Medellin, Colombia

J. Mejia Guisao, F. Ramirez, J.D. Ruiz Alvarez, C.A. Salazar González

University of Split, Faculty of Electrical Engineering, Mechanical Engineering and Naval Architecture, Split, Croatia

D. Giljanovic, N. Godinovic, D. Lelas, I. Puljak

University of Split, Faculty of Science, Split, Croatia

Z. Antunovic, M. Kovac, T. Sculac

Institute Rudjer Boskovic, Zagreb, Croatia

V. Brigljevic, D. Ferencek, D. Majumder, M. Roguljic, A. Starodumov¹¹, T. Susa

University of Cyprus, Nicosia, Cyprus

A. Attikis, K. Christoforou, E. Erodotou, A. Ioannou, G. Kole, M. Kolosova, S. Konstantinou, J. Mousa, C. Nicolaou, F. Ptochos, P.A. Razis, H. Rykaczewski, H. Saka

Charles University, Prague, Czech Republic

M. Finger¹², M. Finger Jr.¹², A. Kveton

Escuela Politecnica Nacional, Quito, Ecuador

E. Ayala

Universidad San Francisco de Quito, Quito, Ecuador

E. Carrera Jarrin

Academy of Scientific Research and Technology of the Arab Republic of Egypt, Egyptian Network of High Energy Physics, Cairo, Egypt

H. Abdalla¹³, Y. Assran^{14,15}

Center for High Energy Physics (CHEP-FU), Fayoum University, El-Fayoum, Egypt

A. Lotfy, M.A. Mahmoud

National Institute of Chemical Physics and Biophysics, Tallinn, Estonia

S. Bhowmik, R.K. Dewanjee, K. Ehataht, M. Kadastik, S. Nandan, C. Nielsen, J. Pata, M. Raidal, L. Tani, C. Veelken

Department of Physics, University of Helsinki, Helsinki, Finland

P. Eerola, L. Forthomme, H. Kirschenmann, K. Osterberg, M. Voutilainen

Helsinki Institute of Physics, Helsinki, Finland

S. Bharthuar, E. Brücken, F. Garcia, J. Havukainen, M.S. Kim, R. Kinnunen, T. Lampén, K. Lassila-Perini, S. Lehti, T. Lindén, M. Lotti, L. Martikainen, M. Myllymäki, J. Ott, H. Siikonen, E. Tuominen, J. Tuominiemi

Lappeenranta University of Technology, Lappeenranta, Finland

P. Luukka, H. Petrow, T. Tuuva

IRFU, CEA, Université Paris-Saclay, Gif-sur-Yvette, France

C. Amendola, M. Besancon, F. Couderc, M. Dejardin, D. Denegri, J.L. Faure, F. Ferri, S. Ganjour, A. Givernaud, P. Gras, G. Hamel de Monchenault, P. Jarry, B. Lenzi, E. Locci, J. Malcles, J. Rander, A. Rosowsky, M.Ö. Sahin, A. Savoy-Navarro¹⁶, M. Titov, G.B. Yu

Laboratoire Leprince-Ringuet, CNRS/IN2P3, Ecole Polytechnique, Institut Polytechnique de Paris, Palaiseau, France

S. Ahuja, F. Beaudette, M. Bonanomi, A. Buchot Perraguin, P. Busson, A. Cappati, C. Charlot, O. Davignon, B. Diab, G. Falmagne, S. Ghosh, R. Granier de Cassagnac, A. Hakimi, I. Kucher, M. Nguyen, C. Ochando, P. Paganini, J. Rembser, R. Salerno, J.B. Sauvan, Y. Sirois, A. Zabi, A. Zghiche

Université de Strasbourg, CNRS, IPHC UMR 7178, Strasbourg, France

J.-L. Agram¹⁷, J. Andrea, D. Apparau, D. Bloch, G. Bourgatte, J.-M. Brom, E.C. Chabert, C. Collard, D. Darej, J.-C. Fontaine¹⁷, U. Goerlach, C. Grimault, A.-C. Le Bihan, E. Nibigira, P. Van Hove

Institut de Physique des 2 Infinis de Lyon (IP2I), Villeurbanne, France

E. Asilar, S. Beauceron, C. Bernet, G. Boudoul, C. Camen, A. Carle, N. Chanon, D. Contardo, P. Depasse, H. El Mamouni, J. Fay, S. Gascon, M. Gouzevitch, B. Ille, I.B. Laktineh, H. Lattaud, A. Lesauvage, M. Lethuillier, L. Mirabito, S. Perries, K. Shchablo, V. Sordini, L. Torterotot, G. Touquet, M. Vander Donckt, S. Viret

Georgian Technical University, Tbilisi, Georgia

I. Lomidze, T. Toriashvili¹⁸, Z. Tsamalaidze¹²

RWTH Aachen University, I. Physikalisches Institut, Aachen, Germany

L. Feld, K. Klein, M. Lipinski, D. Meuser, A. Pauls, M.P. Rauch, N. Röwert, J. Schulz, M. Teroerde

RWTH Aachen University, III. Physikalisches Institut A, Aachen, Germany

A. Dodonova, D. Eliseev, M. Erdmann, P. Fackeldey, B. Fischer, S. Ghosh, T. Hebbeker, K. Hoepfner, F. Ivone, H. Keller, L. Mastrolorenzo, M. Merschmeyer, A. Meyer, G. Mocellin,

S. Mondal, S. Mukherjee, D. Noll, A. Novak, T. Pook, A. Pozdnyakov, Y. Rath, H. Reithler, J. Roemer, A. Schmidt, S.C. Schuler, A. Sharma, L. Vigilante, S. Wiedenbeck, S. Zaleski

RWTH Aachen University, III. Physikalisches Institut B, Aachen, Germany

C. Dziwok, G. Flügge, W. Haj Ahmad¹⁹, O. Hlushchenko, T. Kress, A. Nowack, C. Pistone, O. Pooth, D. Roy, H. Sert, A. Stahl²⁰, T. Ziemons

Deutsches Elektronen-Synchrotron, Hamburg, Germany

H. Aarup Petersen, M. Aldaya Martin, P. Asmuss, I. Babounikau, S. Baxter, O. Behnke, A. Bermúdez Martínez, S. Bhattacharya, A.A. Bin Anuar, K. Borras²¹, V. Botta, D. Brunner, A. Campbell, A. Cardini, C. Cheng, F. Colombina, S. Consuegra Rodríguez, G. Correia Silva, V. Danilov, L. Didukh, G. Eckerlin, D. Eckstein, L.I. Estevez Banos, O. Filatov, E. Gallo²², A. Geiser, A. Giraldi, A. Grohsjean, M. Guthoff, A. Jafari²³, N.Z. Jomhari, H. Jung, A. Kasem²¹, M. Kasemann, H. Kaveh, C. Kleinwort, D. Krücker, W. Lange, J. Lidrych, K. Lipka, W. Lohmann²⁴, R. Mankel, I.-A. Melzer-Pellmann, J. Metwally, A.B. Meyer, M. Meyer, J. Mnich, A. Mussgiller, Y. Otariid, D. Pérez Adán, D. Pitzl, A. Raspereza, B. Ribeiro Lopes, J. Rübenach, A. Saggio, A. Saibel, M. Savitskyi, M. Scham, V. Scheurer, C. Schwanenberger²², A. Singh, R.E. Sosa Ricardo, D. Stafford, N. Tonon, O. Turkot, M. Van De Klundert, R. Walsh, D. Walter, Y. Wen, K. Wichmann, L. Wiens, C. Wissing, S. Wuchterl

University of Hamburg, Hamburg, Germany

R. Aggleton, S. Albrecht, S. Bein, L. Benato, A. Benecke, P. Connor, K. De Leo, M. Eich, F. Feindt, A. Fröhlich, C. Garbers, E. Garutti, P. Gunnellini, J. Haller, A. Hinzmann, G. Kasieczka, R. Klanner, R. Kogler, T. Kramer, V. Kutzner, J. Lange, T. Lange, A. Lobanov, A. Malara, A. Nigamova, K.J. Pena Rodriguez, O. Rieger, P. Schleper, M. Schröder, J. Schwandt, D. Schwarz, J. Sonneveld, H. Stadie, G. Steinbrück, A. Tews, B. Vormwald, I. Zoi

Karlsruher Institut fuer Technologie, Karlsruhe, Germany

J. Bechtel, T. Berger, E. Butz, R. Caspart, T. Chwalek, W. De Boer[†], A. Dierlamm, A. Droll, K. El Morabit, N. Faltermann, M. Giffels, J.o. Gosewisch, A. Gottmann, F. Hartmann²⁰, C. Heidecker, U. Husemann, I. Katkov²⁵, P. Keicher, R. Koppenhöfer, S. Maier, M. Metzler, S. Mitra, Th. Müller, M. Neukum, A. Nürnberg, G. Quast, K. Rabbertz, J. Rauser, D. Savoju, M. Schnepf, D. Seith, I. Shvetsov, H.J. Simonis, R. Ulrich, J. Van Der Linden, R.F. Von Cube, M. Wassmer, M. Weber, S. Wieland, R. Wolf, S. Wozniewski, S. Wunsch

Institute of Nuclear and Particle Physics (INPP), NCSR Demokritos, Aghia Paraskevi, Greece

G. Anagnostou, G. Daskalakis, T. Gerasis, A. Kyriakis, D. Loukas, A. Stakia

National and Kapodistrian University of Athens, Athens, Greece

M. Diamantopoulou, D. Karasavvas, G. Karathanasis, P. Kontaxakis, C.K. Koraka, A. Manousakis-katsikakis, A. Panagiotou, I. Papavergou, N. Saoulidou, K. Theofilatos, E. Tziaferi, K. Vellidis, E. Vourliotis

National Technical University of Athens, Athens, Greece

G. Bakas, K. Kousouris, I. Papakrivopoulos, G. Tsipolitis, A. Zacharopoulou

University of Ioánnina, Ioánnina, Greece

I. Evangelou, C. Foudas, P. Gianneios, P. Katsoulis, P. Kokkas, N. Manthos, I. Papadopoulos, J. Strologas

MTA-ELTE Lendület CMS Particle and Nuclear Physics Group, Eötvös Loránd University

M. Csanad, K. Farkas, M.M.A. Gadallah²⁶, S. Lökös²⁷, P. Major, K. Mandal, A. Mehta, G. Pasztor, A.J. Rádl, O. Surányi, G.I. Veres

Wigner Research Centre for Physics, Budapest, Hungary

M. Bartók²⁸, G. Bencze, C. Hajdu, D. Horvath²⁹, F. Sikler, V. Veszpremi, G. Vesztergombi[†]

Institute of Nuclear Research ATOMKI, Debrecen, Hungary

S. Czellar, J. Karancki²⁸, J. Molnar, Z. Szillasi, D. Teyssier

Institute of Physics, University of Debrecen

P. Raics, Z.L. Trocsanyi³⁰, B. Ujvari

Karoly Robert Campus, MATE Institute of Technology

T. Csorgo³¹, F. Nemes³¹, T. Novak

Indian Institute of Science (IISc), Bangalore, India

J.R. Komaragiri, D. Kumar, L. Panwar, P.C. Tiwari

National Institute of Science Education and Research, HBNI, Bhubaneswar, India

S. Bahinipati³², C. Kar, P. Mal, T. Mishra, V.K. Muraleedharan Nair Bindhu³³, A. Nayak³³, P. Saha, N. Sur, S.K. Swain, D. Vats³³

Panjab University, Chandigarh, India

S. Bansal, S.B. Beri, V. Bhatnagar, G. Chaudhary, S. Chauhan, N. Dhingra³⁴, R. Gupta, A. Kaur, M. Kaur, S. Kaur, P. Kumari, M. Meena, K. Sandeep, J.B. Singh, A.K. Viridi

University of Delhi, Delhi, India

A. Ahmed, A. Bhardwaj, B.C. Choudhary, M. Gola, S. Keshri, A. Kumar, M. Naimuddin, P. Priyanka, K. Ranjan, A. Shah

Saha Institute of Nuclear Physics, HBNI, Kolkata, India

M. Bharti³⁵, R. Bhattacharya, S. Bhattacharya, D. Bhowmik, S. Dutta, S. Dutta, B. Gomber³⁶, M. Maity³⁷, P. Palit, P.K. Rout, G. Saha, B. Sahu, S. Sarkar, M. Sharan, B. Singh³⁵, S. Thakur³⁵

Indian Institute of Technology Madras, Madras, India

P.K. Behera, S.C. Behera, P. Kalbhor, A. Muhammad, R. Pradhan, P.R. Pujahari, A. Sharma, A.K. Sikdar

Bhabha Atomic Research Centre, Mumbai, India

D. Dutta, V. Jha, V. Kumar, D.K. Mishra, K. Naskar³⁸, P.K. Netrakanti, L.M. Pant, P. Shukla

Tata Institute of Fundamental Research-A, Mumbai, India

T. Aziz, S. Dugad, M. Kumar, U. Sarkar

Tata Institute of Fundamental Research-B, Mumbai, India

S. Banerjee, R. Chudasama, M. Guchait, S. Karmakar, S. Kumar, G. Majumder, K. Mazumdar, S. Mukherjee

Indian Institute of Science Education and Research (IISER), Pune, India

K. Alpana, S. Dube, B. Kansal, A. Laha, S. Pandey, A. Rane, A. Rastogi, S. Sharma

Isfahan University of Technology, Isfahan, Iran

H. Bakhshiansohi³⁹, M. Zeinali⁴⁰

Institute for Research in Fundamental Sciences (IPM), Tehran, Iran

S. Chenarani⁴¹, S.M. Etesami, M. Khakzad, M. Mohammadi Najafabadi

University College Dublin, Dublin, Ireland

M. Grunewald

INFN Sezione di Bari ^a, Università di Bari ^b, Politecnico di Bari ^c, Bari, Italy

M. Abbrescia^{a,b}, R. Aly^{a,b,42}, C. Aruta^{a,b}, A. Colaleo^a, D. Creanza^{a,c}, N. De Filippis^{a,c}, M. De Palma^{a,b}, A. Di Florio^{a,b}, A. Di Pilato^{a,b}, W. Elmetenawee^{a,b}, L. Fiore^a, A. Gelmi^{a,b}, M. Gul^a, G. Iaselli^{a,c}, M. Ince^{a,b}, S. Lezki^{a,b}, G. Maggi^{a,c}, M. Maggi^a, I. Margjeka^{a,b}, V. Mastrapasqua^{a,b}, J.A. Merlin^a, S. My^{a,b}, S. Nuzzo^{a,b}, A. Pellecchia^{a,b}, A. Pompili^{a,b}, G. Pugliese^{a,c}, A. Ranieri^a, G. Selvaggi^{a,b}, L. Silvestris^a, F.M. Simone^{a,b}, R. Venditti^a, P. Verwilligen^a

INFN Sezione di Bologna ^a, Università di Bologna ^b, Bologna, Italy

G. Abbiendi^a, C. Battilana^{a,b}, D. Bonacorsi^{a,b}, L. Borgonovi^a, L. Brigliadori^a, R. Campanini^{a,b}, P. Capiluppi^{a,b}, A. Castro^{a,b}, F.R. Cavallo^a, M. Cuffiani^{a,b}, G.M. Dallavalle^a, T. Diotallevi^{a,b}, F. Fabbri^a, A. Fanfani^{a,b}, P. Giacomelli^a, L. Giommi^{a,b}, C. Grandi^a, L. Guiducci^{a,b}, S. Lo Meo^{a,43}, L. Lunerti^{a,b}, S. Marcellini^a, G. Masetti^a, F.L. Navarria^{a,b}, A. Perrotta^a, F. Primavera^{a,b}, A.M. Rossi^{a,b}, T. Rovelli^{a,b}, G.P. Siroli^{a,b}

INFN Sezione di Catania ^a, Università di Catania ^b, Catania, Italy

S. Albergo^{a,b,44}, S. Costa^{a,b,44}, A. Di Mattia^a, R. Potenza^{a,b}, A. Tricomi^{a,b,44}, C. Tuve^{a,b}

INFN Sezione di Firenze ^a, Università di Firenze ^b, Firenze, Italy

G. Barbagli^a, A. Cassese^a, R. Ceccarelli^{a,b}, V. Ciulli^{a,b}, C. Civinini^a, R. D'Alessandro^{a,b}, E. Focardi^{a,b}, G. Latino^{a,b}, P. Lenzi^{a,b}, M. Lizzo^{a,b}, M. Meschini^a, S. Paoletti^a, R. Seidita^{a,b}, G. Sguazzoni^a, L. Viliani^a

INFN Laboratori Nazionali di Frascati, Frascati, Italy

L. Benussi, S. Bianco, D. Piccolo

INFN Sezione di Genova ^a, Università di Genova ^b, Genova, Italy

M. Bozzo^{a,b}, F. Ferro^a, R. Mulargia^{a,b}, E. Robutti^a, S. Tosi^{a,b}

INFN Sezione di Milano-Bicocca ^a, Università di Milano-Bicocca ^b, Milano, Italy

A. Benaglia^a, F. Brivio^{a,b}, F. Cetorelli^{a,b}, V. Ciriolo^{a,b,20}, F. De Guio^{a,b}, M.E. Dinardo^{a,b}, P. Dini^a, S. Gennai^a, A. Ghezzi^{a,b}, P. Govoni^{a,b}, L. Guzzi^{a,b}, M. Malberti^a, S. Malvezzi^a, A. Massironi^a, D. Menasce^a, L. Moroni^a, M. Paganoni^{a,b}, D. Pedrini^a, S. Ragazzi^{a,b}, N. Redaelli^a, T. Tabarelli de Fatis^{a,b}, D. Valsecchi^{a,b,20}, D. Zuolo^{a,b}

INFN Sezione di Napoli ^a, Università di Napoli 'Federico II' ^b, Napoli, Italy, Università della Basilicata ^c, Potenza, Italy, Università G. Marconi ^d, Roma, Italy

S. Buontempo^a, F. Carnevali^{a,b}, N. Cavallo^{a,c}, A. De Iorio^{a,b}, F. Fabozzi^{a,c}, A.O.M. Iorio^{a,b}, L. Lista^{a,b}, S. Meola^{a,d,20}, P. Paolucci^{a,20}, B. Rossi^a, C. Sciacca^{a,b}

INFN Sezione di Padova ^a, Università di Padova ^b, Padova, Italy, Università di Trento ^c, Trento, Italy

P. Azzi^a, N. Bacchetta^a, D. Bisello^{a,b}, P. Bortignon^a, A. Bragagnolo^{a,b}, R. Carlin^{a,b}, P. Checchia^a, T. Dorigo^a, U. Dosselli^a, F. Gasparini^{a,b}, U. Gasparini^{a,b}, S.Y. Hoh^{a,b}, L. Layer^{a,45}, M. Margoni^{a,b}, A.T. Meneguzzo^{a,b}, J. Pazzini^{a,b}, M. Presilla^{a,b}, P. Ronchese^{a,b}, R. Rossin^{a,b}, F. Simonetto^{a,b}, G. Strong^a, M. Tosi^{a,b}, H. YARAR^{a,b}, M. Zanetti^{a,b}, P. Zotto^{a,b}, A. Zucchetta^{a,b}, G. Zumerle^{a,b}

INFN Sezione di Pavia ^a, Università di Pavia ^b

C. Aime^{a,b}, A. Braghieri^a, S. Calzaferri^{a,b}, D. Fiorina^{a,b}, P. Montagna^{a,b}, S.P. Ratti^{a,b}, V. Re^a, C. Riccardi^{a,b}, P. Salvini^a, I. Vai^a, P. Vitulo^{a,b}

INFN Sezione di Perugia ^a, Università di Perugia ^b, Perugia, Italy

P. Asenov^{a,46}, G.M. Bilei^a, D. Ciangottini^{a,b}, L. Fanò^{a,b}, P. Lariccia^{a,b}, M. Magherini^b

G. Mantovani^{a,b}, V. Mariani^{a,b}, M. Menichelli^a, F. Moscatelli^{a,46}, A. Piccinelli^{a,b}, A. Rossi^{a,b}, A. Santocchia^{a,b}, D. Spiga^a, T. Tedeschi^{a,b}

INFN Sezione di Pisa ^a, Università di Pisa ^b, Scuola Normale Superiore di Pisa ^c, Pisa Italy, Università di Siena ^d, Siena, Italy

P. Azzurri^a, G. Bagliesi^a, V. Bertacchi^{a,c}, L. Bianchini^a, T. Boccali^a, E. Bossini^{a,b}, R. Castaldi^a, M.A. Ciocci^{a,b}, V. D'Amante^{a,d}, R. Dell'Orso^a, M.R. Di Domenico^{a,d}, S. Donato^a, A. Giassi^a, F. Ligabue^{a,c}, E. Manca^{a,c}, G. Mandorli^{a,c}, A. Messineo^{a,b}, F. Palla^a, S. Parolia^{a,b}, G. Ramirez-Sanchez^{a,c}, A. Rizzi^{a,b}, G. Rolandi^{a,c}, S. Roy Chowdhury^{a,c}, A. Scribano^a, N. Shafiei^{a,b}, P. Spagnolo^a, R. Tenchini^a, G. Tonelli^{a,b}, N. Turini^{a,d}, A. Venturi^a, P.G. Verdini^a

INFN Sezione di Roma ^a, Sapienza Università di Roma ^b, Rome, Italy

M. Campana^{a,b}, F. Cavallari^a, D. Del Re^{a,b}, E. Di Marco^a, M. Diemoz^a, E. Longo^{a,b}, P. Meridiani^a, G. Organtini^{a,b}, F. Pandolfi^a, R. Paramatti^{a,b}, C. Quaranta^{a,b}, S. Rahatlou^{a,b}, C. Rovelli^a, F. Santanastasio^{a,b}, L. Soffi^a, R. Tramontano^{a,b}

INFN Sezione di Torino ^a, Università di Torino ^b, Torino, Italy, Università del Piemonte Orientale ^c, Novara, Italy

N. Amapane^{a,b}, R. Arcidiacono^{a,c}, S. Argiro^{a,b}, M. Arneodo^{a,c}, N. Bartosik^a, R. Bellan^{a,b}, A. Bellora^{a,b}, J. Berenguer Antequera^{a,b}, C. Biino^a, N. Cartiglia^a, S. Cometti^a, M. Costa^{a,b}, R. Covarelli^{a,b}, N. Demaria^a, B. Kiani^{a,b}, F. Legger^a, C. Mariotti^a, S. Maselli^a, E. Migliore^{a,b}, E. Monteil^{a,b}, M. Monteno^a, M.M. Obertino^{a,b}, G. Ortona^a, L. Pacher^{a,b}, N. Pastrone^a, M. Pelliccioni^a, G.L. Pinna Angioni^{a,b}, M. Ruspa^{a,c}, K. Shchelina^{a,b}, F. Siviero^{a,b}, V. Sola^a, A. Solano^{a,b}, D. Soldi^{a,b}, A. Staiano^a, M. Tornago^{a,b}, D. Trocino^{a,b}, A. Vagnerini

INFN Sezione di Trieste ^a, Università di Trieste ^b, Trieste, Italy

S. Belforte^a, V. Candelise^{a,b}, M. Casarsa^a, F. Cossutti^a, A. Da Rold^{a,b}, G. Della Ricca^{a,b}, G. Sorrentino^{a,b}, F. Vazzoler^{a,b}

Kyungpook National University, Daegu, Korea

S. Dogra, C. Huh, B. Kim, D.H. Kim, G.N. Kim, J. Kim, J. Lee, S.W. Lee, C.S. Moon, Y.D. Oh, S.I. Pak, B.C. Radburn-Smith, S. Sekmen, Y.C. Yang

Chonnam National University, Institute for Universe and Elementary Particles, Kwangju, Korea

H. Kim, D.H. Moon

Hanyang University, Seoul, Korea

B. Francois, T.J. Kim, J. Park

Korea University, Seoul, Korea

S. Cho, S. Choi, Y. Go, B. Hong, K. Lee, K.S. Lee, J. Lim, J. Park, S.K. Park, J. Yoo

Kyung Hee University, Department of Physics, Seoul, Republic of Korea

J. Goh, A. Gurtu

Sejong University, Seoul, Korea

H.S. Kim, Y. Kim

Seoul National University, Seoul, Korea

J. Almond, J.H. Bhyun, J. Choi, S. Jeon, J. Kim, J.S. Kim, S. Ko, H. Kwon, H. Lee, S. Lee, B.H. Oh, M. Oh, S.B. Oh, H. Seo, U.K. Yang, I. Yoon

University of Seoul, Seoul, Korea

W. Jang, D. Jeon, D.Y. Kang, Y. Kang, J.H. Kim, S. Kim, B. Ko, J.S.H. Lee, Y. Lee, I.C. Park, Y. Roh, M.S. Ryu, D. Song, I.J. Watson, S. Yang

Yonsei University, Department of Physics, Seoul, Korea

S. Ha, H.D. Yoo

Sungkyunkwan University, Suwon, Korea

M. Choi, Y. Jeong, H. Lee, Y. Lee, I. Yu

College of Engineering and Technology, American University of the Middle East (AUM), Egaila, Kuwait

T. Beyrouthy, Y. Maghrbi

Riga Technical University

V. Veckalns⁴⁷

Vilnius University, Vilnius, Lithuania

M. Ambrozias, A. Carvalho Antunes De Oliveira, A. Juodagalvis, A. Rinkevicius, G. Tamulaitis

National Centre for Particle Physics, Universiti Malaya, Kuala Lumpur, Malaysia

N. Bin Norjoharuddeen, W.A.T. Wan Abdullah, M.N. Yusli, Z. Zolkapli

Universidad de Sonora (UNISON), Hermosillo, Mexico

J.F. Benitez, A. Castaneda Hernandez, M. León Coello, J.A. Murillo Quijada, A. Sehwawat, L. Valencia Palomo

Centro de Investigacion y de Estudios Avanzados del IPN, Mexico City, Mexico

G. Ayala, H. Castilla-Valdez, E. De La Cruz-Burelo, I. Heredia-De La Cruz⁴⁸, R. Lopez-Fernandez, C.A. Mondragon Herrera, D.A. Perez Navarro, A. Sanchez-Hernandez

Universidad Iberoamericana, Mexico City, Mexico

S. Carrillo Moreno, C. Oropeza Barrera, M. Ramirez-Garcia, F. Vazquez Valencia

Benemerita Universidad Autonoma de Puebla, Puebla, Mexico

I. Pedraza, H.A. Salazar Ibarguen, C. Uribe Estrada

University of Montenegro, Podgorica, Montenegro

J. Mijuskovic⁴⁹, N. Raicevic

University of Auckland, Auckland, New Zealand

D. Krofcheck

University of Canterbury, Christchurch, New Zealand

S. Bheesette, P.H. Butler

National Centre for Physics, Quaid-I-Azam University, Islamabad, Pakistan

A. Ahmad, M.I. Asghar, A. Awais, M.I.M. Awan, H.R. Hoorani, W.A. Khan, M.A. Shah, M. Shoaib, M. Waqas

AGH University of Science and Technology Faculty of Computer Science, Electronics and Telecommunications, Krakow, Poland

V. Avati, L. Grzanka, M. Malawski

National Centre for Nuclear Research, Swierk, Poland

H. Bialkowska, M. Bluj, B. Boimska, M. Górski, M. Kazana, M. Szleper, P. Zalewski

Institute of Experimental Physics, Faculty of Physics, University of Warsaw, Warsaw, Poland
K. Bunkowski, K. Doroba, A. Kalinowski, M. Konecki, J. Krolikowski, M. Walczak

Laboratório de Instrumentação e Física Experimental de Partículas, Lisboa, Portugal
M. Araujo, P. Bargassa, D. Bastos, A. Boletti, P. Faccioli, M. Gallinaro, J. Hollar, N. Leonardo, T. Niknejad, M. Pisano, J. Seixas, O. Toldaiev, J. Varela

Joint Institute for Nuclear Research, Dubna, Russia
S. Afanasiev, D. Budkouski, I. Golutvin, I. Gorbunov, V. Karjavine, V. Korenkov, A. Lanev, A. Malakhov, V. Matveev^{50,51}, V. Palichik, V. Perelygin, M. Savina, D. Seitova, V. Shalaev, S. Shmatov, S. Shulha, V. Smirnov, O. Teryaev, N. Voytishin, B.S. Yuldashev⁵², A. Zarubin, I. Zhizhin

Petersburg Nuclear Physics Institute, Gatchina (St. Petersburg), Russia
G. Gavrillov, V. Golovtsov, Y. Ivanov, V. Kim⁵³, E. Kuznetsova⁵⁴, V. Murzin, V. Oreshkin, I. Smirnov, D. Sosnov, V. Sulimov, L. Uvarov, S. Volkov, A. Vorobyev

Institute for Nuclear Research, Moscow, Russia
Yu. Andreev, A. Dermenev, S. Gninenko, N. Golubev, A. Karneyeu, D. Kirpichnikov, M. Kirsanov, N. Krasnikov, A. Pashenkov, G. Pivovarov, D. Tlisov[†], A. Toropin

Institute for Theoretical and Experimental Physics named by A.I. Alikhanov of NRC 'Kurchatov Institute', Moscow, Russia
V. Epshteyn, V. Gavrillov, N. Lychkovskaya, A. Nikitenko⁵⁵, V. Popov, A. Spiridonov, A. Stepenov, M. Toms, E. Vlasov, A. Zhokin

Moscow Institute of Physics and Technology, Moscow, Russia
T. Aushev

National Research Nuclear University 'Moscow Engineering Physics Institute' (MEPhI), Moscow, Russia
O. Bychkova, M. Chadeeva⁵⁶, P. Parygin, E. Popova, V. Rusinov

P.N. Lebedev Physical Institute, Moscow, Russia
V. Andreev, M. Azarkin, I. Dremin, M. Kirakosyan, A. Terkulov

Skobeltsyn Institute of Nuclear Physics, Lomonosov Moscow State University, Moscow, Russia
A. Belyaev, E. Boos, V. Bunichev, M. Dubinin⁵⁷, L. Dudko, A. Ershov, A. Gribushin, V. Klyukhin, O. Kodolova, I. Lokhtin, S. Obraztsov, M. Perfilov, V. Savrin

Novosibirsk State University (NSU), Novosibirsk, Russia
V. Blinov⁵⁸, T. Dimova⁵⁸, L. Kardapoltsev⁵⁸, A. Kozyrev⁵⁸, I. Ovtin⁵⁸, Y. Skovpen⁵⁸

Institute for High Energy Physics of National Research Centre 'Kurchatov Institute', Protvino, Russia
I. Azhgirey, I. Bayshev, D. Elumakhov, V. Kachanov, D. Konstantinov, P. Mandrik, V. Petrov, R. Ryutin, S. Slabospitskii, A. Sobol, S. Troshin, N. Tyurin, A. Uzunian, A. Volkov

National Research Tomsk Polytechnic University, Tomsk, Russia
A. Babaev, V. Okhotnikov

Tomsk State University, Tomsk, Russia
V. Borshch, V. Ivanchenko, E. Tcherniaev

University of Belgrade: Faculty of Physics and VINCA Institute of Nuclear Sciences, Belgrade, Serbia

P. Adzic⁵⁹, M. Dordevic, P. Milenovic, J. Milosevic

Centro de Investigaciones Energéticas Medioambientales y Tecnológicas (CIEMAT), Madrid, Spain

M. Aguilar-Benitez, J. Alcaraz Maestre, A. Álvarez Fernández, I. Bachiller, M. Barrio Luna, Cristina F. Bedoya, C.A. Carrillo Montoya, M. Cepeda, M. Cerrada, N. Colino, B. De La Cruz, A. Delgado Peris, J.P. Fernández Ramos, J. Flix, M.C. Fouz, O. Gonzalez Lopez, S. Goy Lopez, J.M. Hernandez, M.I. Josa, J. León Holgado, D. Moran, Á. Navarro Tobar, A. Pérez-Calero Yzquierdo, J. Puerta Pelayo, I. Redondo, L. Romero, S. Sánchez Navas, L. Urda Gómez, C. Willmott

Universidad Autónoma de Madrid, Madrid, Spain

J.F. de Trocóniz, R. Reyes-Almanza

Universidad de Oviedo, Instituto Universitario de Ciencias y Tecnologías Espaciales de Asturias (ICTEA), Oviedo, Spain

B. Alvarez Gonzalez, J. Cuevas, C. Erice, J. Fernandez Menendez, S. Folgueras, I. Gonzalez Caballero, J.R. González Fernández, E. Palencia Cortezon, C. Ramón Álvarez, J. Ripoll Sau, V. Rodríguez Bouza, A. Trapote, N. Trevisani

Instituto de Física de Cantabria (IFCA), CSIC-Universidad de Cantabria, Santander, Spain

J.A. Brochero Cifuentes, I.J. Cabrillo, A. Calderon, J. Duarte Campderros, M. Fernandez, C. Fernandez Madrazo, P.J. Fernández Manteca, A. García Alonso, G. Gomez, C. Martinez Rivero, P. Martinez Ruiz del Arbol, F. Matorras, P. Matorras Cuevas, J. Piedra Gomez, C. Prieels, T. Rodrigo, A. Ruiz-Jimeno, L. Scodellaro, I. Vila, J.M. Vizan Garcia

University of Colombo, Colombo, Sri Lanka

MK Jayananda, B. Kailasapathy⁶⁰, D.U.J. Sonnadara, DDC Wickramarathna

University of Ruhuna, Department of Physics, Matara, Sri Lanka

W.G.D. Dharmaratna, K. Liyanage, N. Perera, N. Wickramage

CERN, European Organization for Nuclear Research, Geneva, Switzerland

T.K. Aarrestad, D. Abbaneo, J. Alimena, E. Auffray, G. Auzinger, J. Baechler, P. Baillon[†], D. Barney, J. Bendavid, M. Bianco, A. Bocci, T. Camporesi, M. Capeans Garrido, G. Cerminara, S.S. Chhibra, M. Cipriani, L. Cristella, D. d'Enterria, A. Dabrowski, N. Daci, A. David, A. De Roeck, M.M. Defranchis, M. Deile, M. Dobson, M. Dünser, N. Dupont, A. Elliott-Peisert, N. Emriskova, F. Fallavollita⁶¹, D. Fasanella, S. Fiorendi, A. Florent, G. Franzoni, W. Funk, S. Giani, D. Gigi, K. Gill, F. Glege, L. Gouskos, M. Haranko, J. Hegeman, Y. Iiyama, V. Innocente, T. James, P. Janot, J. Kaspar, J. Kieseler, M. Komm, N. Kratochwil, C. Lange, S. Laurila, P. Lecoq, K. Long, C. Lourenço, L. Malgeri, S. Mallios, M. Mannelli, A.C. Marini, F. Meijers, S. Mersi, E. Meschi, F. Moortgat, M. Mulders, S. Orfanelli, L. Orsini, F. Pantaleo, L. Pape, E. Perez, M. Peruzzi, A. Petrilli, G. Petrucciani, A. Pfeiffer, M. Pierini, D. Piparo, M. Pitt, H. Qu, T. Quast, D. Raby, A. Racz, G. Reales Gutiérrez, M. Rieger, M. Rovere, H. Sakulin, J. Salfeld-Nebgen, S. Scarfi, C. Schäfer, C. Schwick, M. Selvaggi, A. Sharma, P. Silva, W. Snoeys, P. Sphicas⁶², S. Summers, K. Tatar, V.R. Tavolaro, D. Treille, A. Tsiros, G.P. Van Onsem, M. Verzetti, J. Wanczyk⁶³, K.A. Wozniak, W.D. Zeuner

Paul Scherrer Institut, Villigen, Switzerland

L. Caminada⁶⁴, A. Ebrahimi, W. Erdmann, R. Horisberger, Q. Ingram, H.C. Kaestli, D. Kotlinski, U. Langenegger, M. Missiroli, T. Rohe

ETH Zurich - Institute for Particle Physics and Astrophysics (IPA), Zurich, Switzerland

K. Androsov⁶³, M. Backhaus, P. Berger, A. Calandri, N. Chernyavskaya, A. De Cosa, G. Dissertori, M. Dittmar, M. Donegà, C. Dorfer, F. Eble, K. Gedia, F. Glessgen, T.A. Gómez Espinosa, C. Grab, D. Hits, W. Lusterhmann, A.-M. Lyon, R.A. Manzoni, C. Martin Perez, M.T. Meinhard, F. Nessi-Tedaldi, J. Niedziela, F. Pauss, V. Perovic, S. Pigazzini, M.G. Ratti, M. Reichmann, C. Reissel, T. Reitenspiess, B. Ristic, D. Ruini, D.A. Sanz Becerra, M. Schönenberger, V. Stampf, J. Steggemann⁶³, R. Wallny, D.H. Zhu

Universität Zürich, Zurich, Switzerland

C. Amsler⁶⁵, P. Bäertschi, C. Botta, D. Brzhechko, M.F. Canelli, K. Cormier, A. De Wit, R. Del Burgo, J.K. Heikkilä, M. Huwiler, W. Jin, A. Jofrehei, B. Kilminster, S. Leontsinis, S.P. Liechti, A. Macchiolo, P. Meiring, V.M. Mikuni, U. Molinatti, I. Neutelings, A. Reimers, P. Robmann, S. Sanchez Cruz, K. Schweiger, Y. Takahashi

National Central University, Chung-Li, Taiwan

C. Adloff⁶⁶, C.M. Kuo, W. Lin, A. Roy, T. Sarkar³⁷, S.S. Yu

National Taiwan University (NTU), Taipei, Taiwan

L. Ceard, Y. Chao, K.F. Chen, P.H. Chen, W.-S. Hou, Y.y. Li, R.-S. Lu, E. Paganis, A. Psallidas, A. Steen, H.y. Wu, E. Yazgan, P.r. Yu

Chulalongkorn University, Faculty of Science, Department of Physics, Bangkok, Thailand

B. Asavapibhop, C. Asawatangtrakuldee, N. Srimanobhas

Çukurova University, Physics Department, Science and Art Faculty, Adana, Turkey

F. Boran, S. Damarseckin⁶⁷, Z.S. Demiroglu, F. Dolek, I. Dumanoglu⁶⁸, E. Eskut, Y. Guler, E. Gurpinar Guler⁶⁹, I. Hos⁷⁰, C. Isik, O. Kara, A. Kayis Topaksu, U. Kiminsu, G. Onengut, K. Ozdemir⁷¹, A. Polatoz, A.E. Simsek, B. Tali⁷², U.G. Tok, S. Turkcapar, I.S. Zorbakir, C. Zorbilmez

Middle East Technical University, Physics Department, Ankara, Turkey

B. Isildak⁷³, G. Karapinar⁷⁴, K. Ocalan⁷⁵, M. Yalvac⁷⁶

Bogazici University, Istanbul, Turkey

B. Akgun, I.O. Atakisi, E. Gülmez, M. Kaya⁷⁷, O. Kaya⁷⁸, Ö. Özçelik, S. Tekten⁷⁹, E.A. Yetkin⁸⁰

Istanbul Technical University, Istanbul, Turkey

A. Cakir, K. Cankocak⁶⁸, Y. Komurcu, S. Sen⁸¹

Istanbul University, Istanbul, Turkey

S. Cerci⁷², B. Kaynak, S. Ozkorucuklu, D. Sunar Cerci⁷²

Institute for Scintillation Materials of National Academy of Science of Ukraine, Kharkov, Ukraine

B. Grynyov

National Scientific Center, Kharkov Institute of Physics and Technology, Kharkov, Ukraine

L. Levchuk

University of Bristol, Bristol, United Kingdom

D. Anthony, E. Bhal, S. Bologna, J.J. Brooke, A. Bundock, E. Clement, D. Cussans, H. Flacher, J. Goldstein, G.P. Heath, H.F. Heath, M.I. Holmberg⁸², L. Kreczko, B. Krikler, S. Paramesvaran, S. Seif El Nasr-Storey, V.J. Smith, N. Stylianou⁸³, K. Walkingshaw Pass, R. White

Rutherford Appleton Laboratory, Didcot, United Kingdom

K.W. Bell, A. Belyaev⁸⁴, C. Brew, R.M. Brown, D.J.A. Cockerill, C. Cooke, K.V. Ellis, K. Harder,

S. Harper, J. Linacre, K. Manolopoulos, D.M. Newbold, E. Olaiya, D. Petyt, T. Reis, T. Schuh, C.H. Shepherd-Themistocleous, I.R. Tomalin, T. Williams

Imperial College, London, United Kingdom

R. Bainbridge, P. Bloch, S. Bonomally, J. Borg, S. Breeze, O. Buchmuller, V. Cepaitis, G.S. Chahal⁸⁵, D. Colling, P. Dauncey, G. Davies, M. Della Negra, S. Fayer, G. Fedi, G. Hall, M.H. Hassanshahi, G. Iles, J. Langford, L. Lyons, A.-M. Magnan, S. Malik, A. Martelli, D.G. Monk, J. Nash⁸⁶, M. Pesaresi, D.M. Raymond, A. Richards, A. Rose, E. Scott, C. Seez, A. Shtipliyski, A. Tapper, K. Uchida, T. Virdee²⁰, M. Vojinovic, N. Wardle, S.N. Webb, D. Winterbottom, A.G. Zecchinelli

Brunel University, Uxbridge, United Kingdom

K. Coldham, J.E. Cole, A. Khan, P. Kyberd, I.D. Reid, L. Teodorescu, S. Zahid

Baylor University, Waco, USA

S. Abdullin, A. Brinkerhoff, B. Caraway, J. Dittmann, K. Hatakeyama, A.R. Kanuganti, B. McMaster, N. Pastika, M. Saunders, S. Sawant, C. Sutantawibul, J. Wilson

Catholic University of America, Washington, DC, USA

R. Bartek, A. Dominguez, R. Uniyal, A.M. Vargas Hernandez

The University of Alabama, Tuscaloosa, USA

A. Buccilli, S.I. Cooper, D. Di Croce, S.V. Gleyzer, C. Henderson, C.U. Perez, P. Rumerio⁸⁷, C. West

Boston University, Boston, USA

A. Akpınar, A. Albert, D. Arcaro, C. Cosby, Z. Demiragli, E. Fontanesi, D. Gastler, J. Rohlf, K. Salyer, D. Sperka, D. Spitzbart, I. Suarez, A. Tsatsos, S. Yuan, D. Zou

Brown University, Providence, USA

G. Benelli, B. Burkley, X. Coubez²¹, D. Cutts, M. Hadley, U. Heintz, J.M. Hogan⁸⁸, G. Landsberg, K.T. Lau, M. Lukasik, J. Luo, M. Narain, S. Sagir⁸⁹, E. Usai, W.Y. Wong, X. Yan, D. Yu, W. Zhang

University of California, Davis, Davis, USA

J. Bonilla, C. Brainerd, R. Breedon, M. Calderon De La Barca Sanchez, M. Chertok, J. Conway, P.T. Cox, R. Erbacher, G. Haza, F. Jensen, O. Kukral, R. Lander, M. Mulhearn, D. Pellett, B. Regnery, D. Taylor, Y. Yao, F. Zhang

University of California, Los Angeles, USA

M. Bachtis, R. Cousins, A. Datta, D. Hamilton, J. Hauser, M. Ignatenko, M.A. Iqbal, T. Lam, W.A. Nash, S. Regnard, D. Saltzberg, B. Stone, V. Valuev

University of California, Riverside, Riverside, USA

K. Burt, Y. Chen, R. Clare, J.W. Gary, M. Gordon, G. Hanson, G. Karapostoli, O.R. Long, N. Manganello, M. Olmedo Negrete, W. Si, S. Wimpenny, Y. Zhang

University of California, San Diego, La Jolla, USA

J.G. Branson, P. Chang, S. Cittolin, S. Cooperstein, N. Deelen, D. Diaz, J. Duarte, R. Gerosa, L. Giannini, D. Gilbert, J. Guiang, R. Kansal, V. Krutelyov, R. Lee, J. Letts, M. Masciovecchio, S. May, M. Pieri, B.V. Sathia Narayanan, V. Sharma, M. Tadel, A. Vartak, F. Würthwein, Y. Xiang, A. Yagil

University of California, Santa Barbara - Department of Physics, Santa Barbara, USA

N. Amin, C. Campagnari, M. Citron, A. Dorsett, V. Dutta, J. Incandela, M. Kilpatrick, J. Kim, B. Marsh, H. Mei, M. Oshiro, M. Quinnan, J. Richman, U. Sarica, J. Sheplock, D. Stuart, S. Wang

California Institute of Technology, Pasadena, USA

A. Bornheim, O. Cerri, I. Dutta, J.M. Lawhorn, N. Lu, J. Mao, H.B. Newman, T.Q. Nguyen, M. Spiropulu, J.R. Vlimant, C. Wang, S. Xie, Z. Zhang, R.Y. Zhu

Carnegie Mellon University, Pittsburgh, USA

J. Alison, S. An, M.B. Andrews, P. Bryant, T. Ferguson, A. Harilal, C. Liu, T. Mudholkar, M. Paulini, A. Sanchez, W. Terrill

University of Colorado Boulder, Boulder, USA

J.P. Cumalat, W.T. Ford, A. Hassani, E. MacDonald, R. Patel, A. Perloff, C. Savard, K. Stenson, K.A. Ulmer, S.R. Wagner

Cornell University, Ithaca, USA

J. Alexander, S. Bright-thonney, Y. Cheng, D.J. Cranshaw, S. Hogan, J. Monroy, J.R. Patterson, D. Quach, J. Reichert, M. Reid, A. Ryd, W. Sun, J. Thom, P. Wittich, R. Zou

Fermi National Accelerator Laboratory, Batavia, USA

M. Albrow, M. Alyari, G. Apollinari, A. Apresyan, A. Apyan, S. Banerjee, L.A.T. Bauerdick, D. Berry, J. Berryhill, P.C. Bhat, K. Burkett, J.N. Butler, A. Canepa, G.B. Cerati, H.W.K. Cheung, F. Chlebana, M. Cremonesi, K.F. Di Petrillo, V.D. Elvira, Y. Feng, J. Freeman, Z. Gecse, L. Gray, D. Green, S. Grünendahl, O. Gutsche, R.M. Harris, R. Heller, T.C. Herwig, J. Hirschauer, B. Jayatilaka, S. Jindariani, M. Johnson, U. Joshi, T. Klijnsma, B. Klima, K.H.M. Kwok, S. Lammel, D. Lincoln, R. Lipton, T. Liu, C. Madrid, K. Maeshima, C. Mantilla, D. Mason, P. McBride, P. Merkel, S. Mrenna, S. Nahn, J. Ngadiuba, V. O'Dell, V. Papadimitriou, K. Pedro, C. Pena⁵⁷, O. Prokofyev, F. Ravera, A. Reinsvold Hall, L. Ristori, B. Schneider, E. Sexton-Kennedy, N. Smith, A. Soha, W.J. Spalding, L. Spiegel, S. Stoynev, J. Strait, L. Taylor, S. Tkaczyk, N.V. Tran, L. Uplegger, E.W. Vaandering, H.A. Weber

University of Florida, Gainesville, USA

D. Acosta, P. Avery, D. Bourilkov, L. Cadamuro, V. Cherepanov, F. Errico, R.D. Field, D. Guerrero, B.M. Joshi, M. Kim, E. Koenig, J. Konigsberg, A. Korytov, K.H. Lo, K. Matchev, N. Menendez, G. Mitselmakher, A. Muthirakalayil Madhu, N. Rawal, D. Rosenzweig, S. Rosenzweig, K. Shi, J. Sturdy, J. Wang, E. Yigitbasi, X. Zuo

Florida State University, Tallahassee, USA

T. Adams, A. Askew, R. Habibullah, V. Hagopian, K.F. Johnson, R. Khurana, T. Kolberg, G. Martinez, H. Prosper, C. Schiber, O. Viazlo, R. Yohay, J. Zhang

Florida Institute of Technology, Melbourne, USA

M.M. Baarmand, S. Butalla, T. Elkafrawy⁹⁰, M. Hohlmann, R. Kumar Verma, D. Noonan, M. Rahmani, F. Yumiceva

University of Illinois at Chicago (UIC), Chicago, USA

M.R. Adams, H. Becerril Gonzalez, R. Cavanaugh, X. Chen, S. Dittmer, O. Evdokimov, C.E. Gerber, D.A. Hangal, D.J. Hofman, A.H. Merrit, C. Mills, G. Oh, T. Roy, S. Rudrabhatla, M.B. Tonjes, N. Varelas, J. Viinikainen, X. Wang, Z. Wu, Z. Ye

The University of Iowa, Iowa City, USA

M. Alhusseini, K. Dilsiz⁹¹, R.P. Gandrajula, O.K. Köseyan, J.-P. Merlo, A. Mestvirishvili⁹², J. Nachtman, H. Ogul⁹³, Y. Onel, A. Penzo, C. Snyder, E. Tiras⁹⁴

Johns Hopkins University, Baltimore, USA

O. Amram, B. Blumenfeld, L. Corcodilos, J. Davis, M. Eminizer, A.V. Gritsan, S. Kyriacou, P. Maksimovic, J. Roskes, M. Swartz, T.Á. Vámi

The University of Kansas, Lawrence, USA

A. Abreu, J. Anguiano, C. Baldenegro Barrera, P. Baringer, A. Bean, A. Bylinkin, Z. Flowers, T. Isidori, S. Khalil, J. King, G. Krintiras, A. Kropivnitskaya, M. Lazarovits, C. Lindsey, J. Marquez, N. Minafra, M. Murray, M. Nickel, C. Rogan, C. Royon, R. Salvatico, S. Sanders, E. Schmitz, C. Smith, J.D. Tapia Takaki, Q. Wang, Z. Warner, J. Williams, G. Wilson

Kansas State University, Manhattan, USA

S. Duric, A. Ivanov, K. Kaadze, D. Kim, Y. Maravin, T. Mitchell, A. Modak, K. Nam

Lawrence Livermore National Laboratory, Livermore, USA

F. Rebassoo, D. Wright

University of Maryland, College Park, USA

E. Adams, A. Baden, O. Baron, A. Belloni, S.C. Eno, N.J. Hadley, S. Jabeen, R.G. Kellogg, T. Koeth, A.C. Mignerey, S. Nabili, C. Palmer, M. Seidel, A. Skuja, L. Wang, K. Wong

Massachusetts Institute of Technology, Cambridge, USA

D. Abercrombie, G. Andreassi, R. Bi, S. Brandt, W. Busza, I.A. Cali, Y. Chen, M. D'Alfonso, J. Eysermans, C. Freer, G. Gomez Ceballos, M. Goncharov, P. Harris, M. Hu, M. Klute, D. Kovalskyi, J. Krupa, Y.-J. Lee, B. Maier, C. Mironov, C. Paus, D. Rankin, C. Roland, G. Roland, Z. Shi, G.S.F. Stephans, J. Wang, Z. Wang, B. Wyslouch

University of Minnesota, Minneapolis, USA

R.M. Chatterjee, A. Evans, P. Hansen, J. Hiltbrand, Sh. Jain, M. Krohn, Y. Kubota, J. Mans, M. Revering, R. Rusack, R. Saradhy, N. Schroeder, N. Strobbe, M.A. Wadud

University of Nebraska-Lincoln, Lincoln, USA

K. Bloom, M. Bryson, S. Chauhan, D.R. Claes, C. Fangmeier, L. Finco, F. Golf, C. Joo, I. Kravchenko, M. Musich, I. Reed, J.E. Siado, G.R. Snow[†], W. Tabb, F. Yan

State University of New York at Buffalo, Buffalo, USA

G. Agarwal, H. Bandyopadhyay, L. Hay, I. Iashvili, A. Kharchilava, C. McLean, D. Nguyen, J. Pekkanen, S. Rappoccio, A. Williams

Northeastern University, Boston, USA

G. Alverson, E. Barberis, Y. Haddad, A. Hortiangtham, J. Li, G. Madigan, B. Marzocchi, D.M. Morse, V. Nguyen, T. Orimoto, A. Parker, L. Skinnari, A. Tishelman-Charny, T. Wamorkar, B. Wang, A. Wisecarver, D. Wood

Northwestern University, Evanston, USA

S. Bhattacharya, J. Bueghly, Z. Chen, A. Gilbert, T. Gunter, K.A. Hahn, Y. Liu, N. Odell, M.H. Schmitt, M. Velasco

University of Notre Dame, Notre Dame, USA

R. Band, R. Bucci, A. Das, N. Dev, R. Goldouzian, M. Hildreth, K. Hurtado Anampa, C. Jessop, K. Lannon, J. Lawrence, N. Loukas, D. Lutton, N. Marinelli, I. Mcalister, T. McCauley, F. Meng, K. Mohrman, Y. Musienko⁵⁰, R. Ruchti, P. Siddireddy, A. Townsend, M. Wayne, A. Wightman, M. Wolf, M. Zarucki, L. Zygala

The Ohio State University, Columbus, USA

B. Bylsma, B. Cardwell, L.S. Durkin, B. Francis, C. Hill, M. Nunez Ornelas, K. Wei, B.L. Winer, B.R. Yates

Princeton University, Princeton, USA

F.M. Addesa, B. Bonham, P. Das, G. Dezoort, P. Elmer, A. Frankenthal, B. Greenberg,

N. Haubrich, S. Higginbotham, A. Kalogeropoulos, G. Kopp, S. Kwan, D. Lange, M.T. Lucchini, D. Marlow, K. Mei, I. Ojalvo, J. Olsen, D. Stickland, C. Tully

University of Puerto Rico, Mayaguez, USA

S. Malik, S. Norberg

Purdue University, West Lafayette, USA

A.S. Bakshi, V.E. Barnes, R. Chawla, S. Das, L. Gutay, M. Jones, A.W. Jung, S. Karmarkar, M. Liu, G. Negro, N. Neumeister, G. Paspalaki, C.C. Peng, S. Piperov, A. Purohit, J.F. Schulte, M. Stojanovic¹⁶, J. Thieman, F. Wang, R. Xiao, W. Xie

Purdue University Northwest, Hammond, USA

J. Dolen, N. Parashar

Rice University, Houston, USA

A. Baty, M. Decaro, S. Dildick, K.M. Ecklund, S. Freed, P. Gardner, F.J.M. Geurts, A. Kumar, W. Li, B.P. Padley, R. Redjimi, W. Shi, A.G. Stahl Leitton, S. Yang, L. Zhang, Y. Zhang

University of Rochester, Rochester, USA

A. Bodek, P. de Barbaro, R. Demina, J.L. Dulemba, C. Fallon, T. Ferbel, M. Galanti, A. Garcia-Bellido, O. Hindrichs, A. Khukhunaishvili, E. Ranken, R. Taus

Rutgers, The State University of New Jersey, Piscataway, USA

B. Chiarito, J.P. Chou, A. Gandrakota, Y. Gershtein, E. Halkiadakis, A. Hart, M. Heindl, O. Karacheban²⁴, I. Laflotte, A. Lath, R. Montalvo, K. Nash, M. Osherson, S. Salur, S. Schnetzer, S. Somalwar, R. Stone, S.A. Thayil, S. Thomas, H. Wang

University of Tennessee, Knoxville, USA

H. Acharya, A.G. Delannoy, S. Spanier

Texas A&M University, College Station, USA

O. Bouhali⁹⁵, M. Dalchenko, A. Delgado, R. Eusebi, J. Gilmore, T. Huang, T. Kamon⁹⁶, H. Kim, S. Luo, S. Malhotra, R. Mueller, D. Overton, D. Rathjens, A. Safonov

Texas Tech University, Lubbock, USA

N. Akchurin, J. Damgov, V. Hegde, S. Kunori, K. Lamichhane, S.W. Lee, T. Mengke, S. Muthumuni, T. Peltola, I. Volobouev, Z. Wang, A. Whitbeck

Vanderbilt University, Nashville, USA

E. Appelt, S. Greene, A. Gurrola, W. Johns, A. Melo, H. Ni, K. Padeken, F. Romeo, P. Sheldon, S. Tuo, J. Velkovska

University of Virginia, Charlottesville, USA

M.W. Arenton, B. Cox, G. Cummings, J. Hakala, R. Hirosky, M. Joyce, A. Ledovskoy, A. Li, C. Neu, B. Tannenwald, E. Wolfe

Wayne State University, Detroit, USA

N. Poudyal

University of Wisconsin - Madison, Madison, WI, USA

K. Black, T. Bose, J. Buchanan, C. Caillol, S. Dasu, I. De Bruyn, P. Everaerts, F. Fienga, C. Galloni, H. He, M. Herndon, A. Hervé, U. Hussain, A. Lanaro, A. Loeliger, R. Loveless, J. Madhusudanan Sreekala, A. Mallampalli, A. Mohammadi, D. Pinna, A. Savin, V. Shang, V. Sharma, W.H. Smith, D. Teague, S. Trembath-reichert, W. Vetens

†: Deceased

- 1: Also at TU Wien, Wien, Austria
- 2: Also at Institute of Basic and Applied Sciences, Faculty of Engineering, Arab Academy for Science, Technology and Maritime Transport, Alexandria, Egypt
- 3: Also at Université Libre de Bruxelles, Bruxelles, Belgium
- 4: Also at Universidade Estadual de Campinas, Campinas, Brazil
- 5: Also at Federal University of Rio Grande do Sul, Porto Alegre, Brazil
- 6: Also at University of Chinese Academy of Sciences, Beijing, China
- 7: Also at Department of Physics, Tsinghua University, Beijing, China
- 8: Also at UFMS, Nova Andradina, Brazil
- 9: Also at Nanjing Normal University Department of Physics, Nanjing, China
- 10: Now at The University of Iowa, Iowa City, USA
- 11: Also at Institute for Theoretical and Experimental Physics named by A.I. Alikhanov of NRC 'Kurchatov Institute', Moscow, Russia
- 12: Also at Joint Institute for Nuclear Research, Dubna, Russia
- 13: Also at Cairo University, Cairo, Egypt
- 14: Also at Suez University, Suez, Egypt
- 15: Now at British University in Egypt, Cairo, Egypt
- 16: Also at Purdue University, West Lafayette, USA
- 17: Also at Université de Haute Alsace, Mulhouse, France
- 18: Also at Tbilisi State University, Tbilisi, Georgia
- 19: Also at Erzincan Binali Yildirim University, Erzincan, Turkey
- 20: Also at CERN, European Organization for Nuclear Research, Geneva, Switzerland
- 21: Also at RWTH Aachen University, III. Physikalisches Institut A, Aachen, Germany
- 22: Also at University of Hamburg, Hamburg, Germany
- 23: Also at Isfahan University of Technology, Isfahan, Iran, Isfahan, Iran
- 24: Also at Brandenburg University of Technology, Cottbus, Germany
- 25: Also at Skobeltsyn Institute of Nuclear Physics, Lomonosov Moscow State University, Moscow, Russia
- 26: Also at Physics Department, Faculty of Science, Assiut University, Assiut, Egypt
- 27: Also at Karoly Robert Campus, MATE Institute of Technology, Gyongyos, Hungary
- 28: Also at Institute of Physics, University of Debrecen, Debrecen, Hungary
- 29: Also at Institute of Nuclear Research ATOMKI, Debrecen, Hungary
- 30: Also at MTA-ELTE Lendület CMS Particle and Nuclear Physics Group, Eötvös Loránd University, Budapest, Hungary
- 31: Also at Wigner Research Centre for Physics, Budapest, Hungary
- 32: Also at IIT Bhubaneswar, Bhubaneswar, India
- 33: Also at Institute of Physics, Bhubaneswar, India
- 34: Also at G.H.G. Khalsa College, Punjab, India
- 35: Also at Shoolini University, Solan, India
- 36: Also at University of Hyderabad, Hyderabad, India
- 37: Also at University of Visva-Bharati, Santiniketan, India
- 38: Also at Indian Institute of Technology (IIT), Mumbai, India
- 39: Also at Deutsches Elektronen-Synchrotron, Hamburg, Germany
- 40: Also at Sharif University of Technology, Tehran, Iran
- 41: Also at Department of Physics, University of Science and Technology of Mazandaran, Behshahr, Iran
- 42: Now at INFN Sezione di Bari ^a, Università di Bari ^b, Politecnico di Bari ^c, Bari, Italy
- 43: Also at Italian National Agency for New Technologies, Energy and Sustainable Economic

Development, Bologna, Italy

44: Also at Centro Siciliano di Fisica Nucleare e di Struttura Della Materia, Catania, Italy

45: Also at Università di Napoli 'Federico II', Napoli, Italy

46: Also at Consiglio Nazionale delle Ricerche - Istituto Officina dei Materiali, PERUGIA, Italy

47: Also at Riga Technical University, Riga, Latvia

48: Also at Consejo Nacional de Ciencia y Tecnología, Mexico City, Mexico

49: Also at IRFU, CEA, Université Paris-Saclay, Gif-sur-Yvette, France

50: Also at Institute for Nuclear Research, Moscow, Russia

51: Now at National Research Nuclear University 'Moscow Engineering Physics Institute' (MEPhI), Moscow, Russia

52: Also at Institute of Nuclear Physics of the Uzbekistan Academy of Sciences, Tashkent, Uzbekistan

53: Also at St. Petersburg State Polytechnical University, St. Petersburg, Russia

54: Also at University of Florida, Gainesville, USA

55: Also at Imperial College, London, United Kingdom

56: Also at P.N. Lebedev Physical Institute, Moscow, Russia

57: Also at California Institute of Technology, Pasadena, USA

58: Also at Budker Institute of Nuclear Physics, Novosibirsk, Russia

59: Also at Faculty of Physics, University of Belgrade, Belgrade, Serbia

60: Also at Trincomalee Campus, Eastern University, Sri Lanka, Nilaveli, Sri Lanka

61: Also at INFN Sezione di Pavia ^a, Università di Pavia ^b, Pavia, Italy

62: Also at National and Kapodistrian University of Athens, Athens, Greece

63: Also at Ecole Polytechnique Fédérale Lausanne, Lausanne, Switzerland

64: Also at Universität Zürich, Zurich, Switzerland

65: Also at Stefan Meyer Institute for Subatomic Physics, Vienna, Austria

66: Also at Laboratoire d'Annecy-le-Vieux de Physique des Particules, IN2P3-CNRS, Annecy-le-Vieux, France

67: Also at Şırnak University, Sırnak, Turkey

68: Also at Near East University, Research Center of Experimental Health Science, Nicosia, Turkey

69: Also at Konya Technical University, Konya, Turkey

70: Also at Istanbul University - Cerrahpasa, Faculty of Engineering, Istanbul, Turkey

71: Also at Piri Reis University, Istanbul, Turkey

72: Also at Adiyaman University, Adiyaman, Turkey

73: Also at Ozyegin University, Istanbul, Turkey

74: Also at Izmir Institute of Technology, Izmir, Turkey

75: Also at Necmettin Erbakan University, Konya, Turkey

76: Also at Bozok Universititesi Rektörlüğü, Yozgat, Turkey

77: Also at Marmara University, Istanbul, Turkey

78: Also at Milli Savunma University, Istanbul, Turkey

79: Also at Kafkas University, Kars, Turkey

80: Also at Istanbul Bilgi University, Istanbul, Turkey

81: Also at Hacettepe University, Ankara, Turkey

82: Also at Rutherford Appleton Laboratory, Didcot, United Kingdom

83: Also at Vrije Universiteit Brussel, Brussel, Belgium

84: Also at School of Physics and Astronomy, University of Southampton, Southampton, United Kingdom

85: Also at IPPP Durham University, Durham, United Kingdom

86: Also at Monash University, Faculty of Science, Clayton, Australia

- 87: Also at Università di Torino, TORINO, Italy
- 88: Also at Bethel University, St. Paul, Minneapolis, USA, St. Paul, USA
- 89: Also at Karamanoğlu Mehmetbey University, Karaman, Turkey
- 90: Also at Ain Shams University, Cairo, Egypt
- 91: Also at Bingol University, Bingol, Turkey
- 92: Also at Georgian Technical University, Tbilisi, Georgia
- 93: Also at Sinop University, Sinop, Turkey
- 94: Also at Erciyes University, KAYSERI, Turkey
- 95: Also at Texas A&M University at Qatar, Doha, Qatar
- 96: Also at Kyungpook National University, Daegu, Korea, Daegu, Korea